


Review

Research Status and Prospective Properties of the Al-Zn-Mg-Cu Series Aluminum Alloys

Jue Wang and Faguo Li * 

School of Materials Science and Engineering, Xiangtan University, Xiangtan 411105, China;
wj200204032022@163.com

* Correspondence: lifaguo@xtu.edu.cn

Abstract: An Al-Zn-Mg-Cu alloy has high specific strength, good corrosion resistance, fracture toughness and fatigue resistance. It is one of the most important structural materials in the fields of aviation, aerospace, weapons and transportation; in particular, it plays a huge role in the field of aerospace. In order to optimize the strength, toughness and corrosion properties of an Al-Zn-Mg-Cu alloy, the focus of research on this alloy has always been on the alloying process. The effects of the main alloying elements, trace alloying elements and rare earth elements on the microstructure and properties of Al-Zn-Mg-Cu alloys are briefly introduced in this paper, and future research directions are proposed.

Keywords: Al-Zn-Mg-Cu alloy; main alloy elements; microalloy elements; rare earth element; performance optimization



Citation: Wang, J.; Li, F. Research Status and Prospective Properties of the Al-Zn-Mg-Cu Series Aluminum Alloys. *Metals* **2023**, *13*, 1329. <https://doi.org/10.3390/met13081329>

Academic Editor: Babak Shalchi Amirkhiz

Received: 14 June 2023
Revised: 13 July 2023
Accepted: 20 July 2023
Published: 25 July 2023



Copyright: © 2023 by the authors. Licensee MDPI, Basel, Switzerland. This article is an open access article distributed under the terms and conditions of the Creative Commons Attribution (CC BY) license (<https://creativecommons.org/licenses/by/4.0/>).

1. Introduction

The main elements of an Al-Zn-Mg-Cu alloy include Al, Zn, Mg and Cu; this alloy also contains trace amounts of Si and Fe (usually present as impurity elements). The types and contents of trace elements are different among different brands, which leads to different aluminum alloys having different mechanical properties. Therefore, the mechanical properties of the Al-Zn-Mg-Cu alloy could be improved by adjusting its composition, selectively introducing trace alloying elements, reducing the impurity content and realizing the reasonable distribution of the precipitate phase. Rare earth elements play a more significant role in this process due to their special electronic structure and chemical properties. However, with the increase in types of alloying elements within an alloy, the phase composition and precipitation behavior of the alloy become more complex. The component differences in local areas are significant. The corrosion cracking sensitivity increases and the contradiction between strength and corrosion performance becomes more acute. Therefore, the influence mechanisms of different elements on the properties of the alloy are discussed, and the range of action and best content of elements are researched in order to solve the contradiction between the strength, toughness and corrosion resistance of aluminum alloy. This is an urgent problem to be solved in the development process of ultra-high-strength aluminum alloy.

2. Main Alloying Elements

The main alloying elements in an Al-Zn-Mg-Cu alloy are Al, Zn, Mg and Cu. The MgZn₂ phase is the main strengthening phase in aluminum alloy. An increase in Zn and Mg elements can improve the yield strength of the alloy. Cu provides a certain contribution to the strength of the alloy that improves the corrosion resistance [1,2]. But there is a threshold for each element, for which the difference is obvious for different components of the alloy.

2.1. Cu

2.1.1. Effect of Different Cu Contents on an Al-Zn-Mg-Cu Alloy

Cu has a certain strengthening effect in Al-Zn-Mg-Cu alloys that has a prominent effect on their corrosion resistance. The addition of Cu can improve the age-hardening potential of the alloy and increase the density of the precipitated strengthened phase [3]. However, when excessive copper was added to a 7055 aluminum alloy, the grain size gradually increased and the alloy performance decreased (Figure 1) [4]. Therefore, reducing the contents of Cu within a certain range was conducive to the diffusion of more Zn and Mg into the matrix, which increased the volume fraction of the strengthening phase $Mg(Zn,Al,Cu)_2$, thus improving the yield strength (YS) and hardness of the alloy.

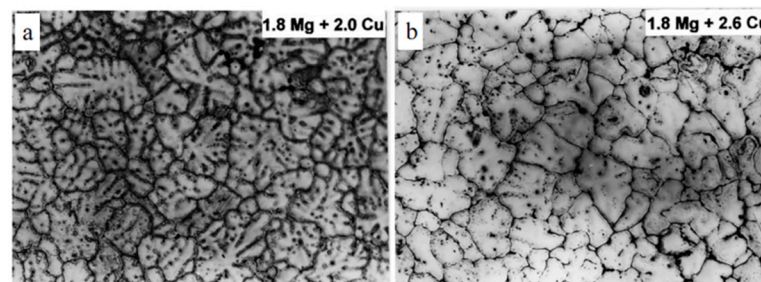


Figure 1. Optical micrographs of as-cast 7055 Al alloys showing cored dendritic microstructures: (a) 1.8 wt.% Mg + 2.0 wt.% Cu; (b) 1.8 wt.% Mg + 2.6 wt.% Cu (Reprinted with permission from Ref. [4]. 2023 Elsevier).

2.1.2. Effect of Cu on Alloys at Different Zn/Mg Ratios

The effect of Cu on the properties of an Al-Zn-Mg-Cu alloy is related to the alloy's composition. In low Zn/Mg ratio alloys (such as type 7050), the addition of Cu increases the amount of reinforced precipitate phase and improves the yield strength and corrosion resistance of the alloy. However, in an Al-9.3Zn-2.4Mg-xCu-0.16Zr aluminum alloy with a high Zn/Mg ratio, when copper content was decreased from 2.2% to 1.8% (mass fraction), the mechanical properties of the alloy and the resistance to spalling corrosion also significantly improved. When the Cu content was reduced to 0.8% (mass fraction), the potential difference between the grain boundary and Al matrix became larger, which resulted in corrosion of the precipitate phase and significantly deteriorated the corrosion performance (Figure 2b) [5].

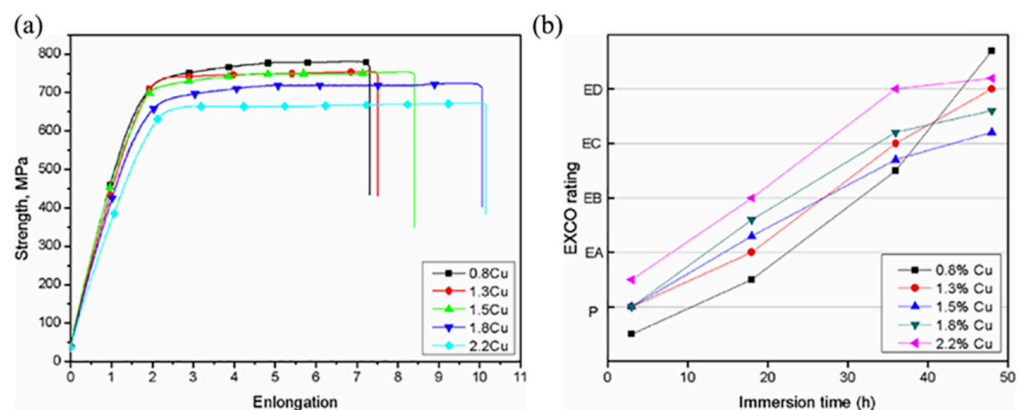


Figure 2. Stress-strain curves (a) of Al-9.3Zn-2.4Mg-xCu-Zr alloy and evolution of the EXCO rating as a function of immersion time for the alloys in the T6 heat treatment (b) (Reprinted with permission from Ref. [5]. 2023 Elsevier).

2.1.3. Effect of Cu in a Highly Alloyed Al-Zn-Mg-Cu Alloy

In a highly alloyed Al-Zn-Mg-Cu alloy, the influence of Cu on the comprehensive properties includes grain refinement and coupling effect of residual eutectic phase. In Al-10.0Zn-2.6Mg-xCu-0.15Zr alloys, on one hand, the volume fraction of the second phase increased significantly with the increase in Cu content. On the other hand, the low diffusion coefficient of Cu inhibited the dissolution of the second phase, which gradually increased the volume fraction of the residual eutectic phase after a solid solution treatment. In the hard and brittle residual eutectic phase, stress concentration easily occurred and it became a crack source, which seriously damaged the plasticity of the alloy. For an Al-10.0Zn-2.6Mg-1.0Cu alloy with $x = 1.0$, the precipitate phase was small and the volume fraction was large (Figure 3), which exhibited the best mechanical properties [6].

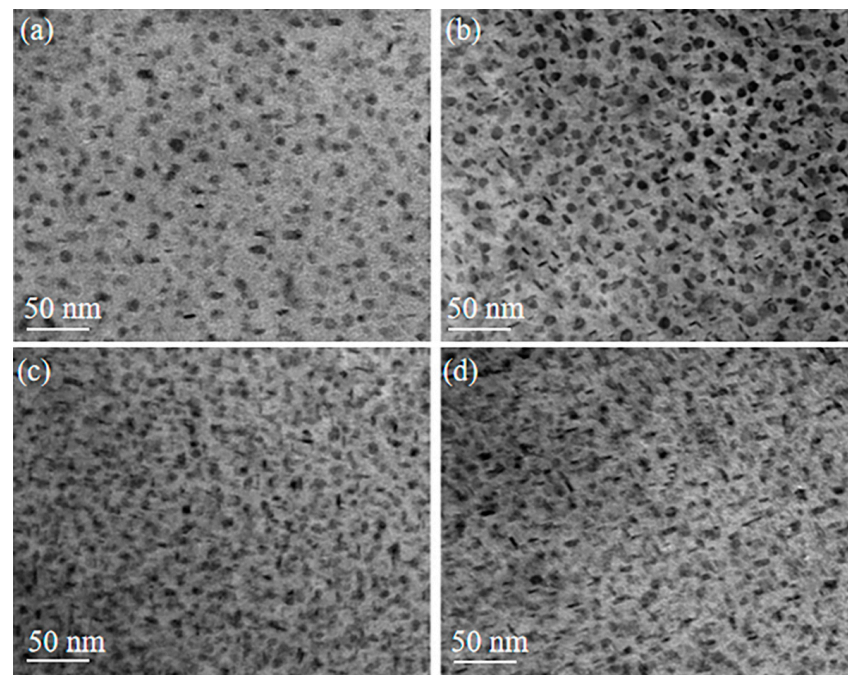


Figure 3. Bright-field TEM images for T6: (a) 0 wt.% Cu, (b) 1.0 wt.% Cu, (c) 2.0 wt.% Cu, (d) 3.0 wt.% Cu (Reprinted with permission from Ref. [6]. 2023 Elsevier).

2.2. Mg

Mg is the main strengthening element of an Al-Zn-Mg-Cu alloy. η (MgZn_2) phase that is formed by Mg and Zn has a large solid solubility in the matrix. The solid solubility decreases significantly with the decrease in temperature, which have a strong age-hardening ability and was the main strengthening phase of the Al-Zn-Mg-Cu alloy. With the increase in Mg content, α (Al) grains were refined (Figure 4) and the tertiary dendrites and the T(AlCuMgZn) phases increased [7]. In addition, the increase in Mg content could improve the volume fraction of the precipitate phase during aging treatment, thus improving the yield strength [8]. However, high yield stress could also lead to lower deformation resistance at grain boundaries, thus promoting intergranular fracture and reducing plasticity [9].

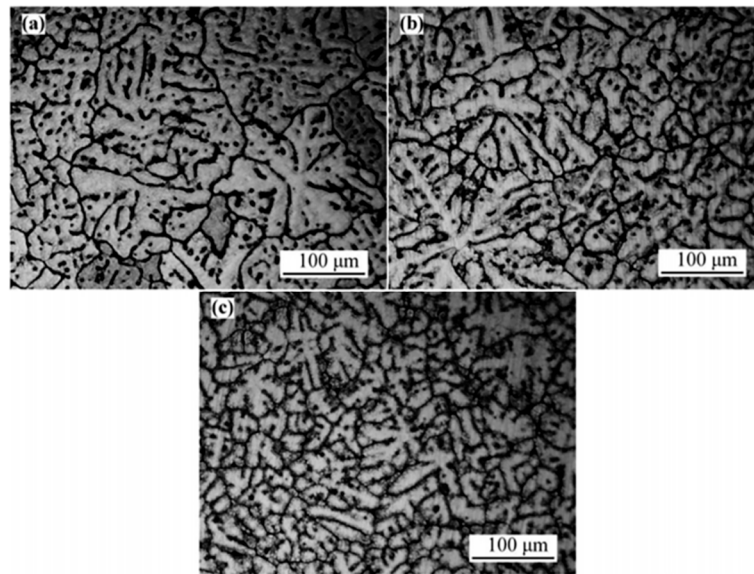


Figure 4. Optical microstructures of as-cast alloys: (a) 2.21 wt.% Mg; (b) 2.76 wt.% Mg; (c) 3.66 wt.% Mg (Reprinted with permission from Ref. [7]. 2023 Elsevier).

2.3. Zn

2.3.1. Effect of Different Zn Contents on Al-Zn-Mg-Cu Alloys

In an Al-Zn-Mg-Cu alloy, increasing the Zn content can promote the nucleation, growth and phase precipitation transformation of the alloy. Al-Zn-Mg-Cu alloys with high Zn content had high precipitation density and fast precipitation rate, which had the advantages of improving the alloy strength and shortening the peak aging time [10]. When the Zn content increased from 4.4% (mass fraction) to 7.2% (mass fraction), the ultimate tensile strength (UTS) of the Al- x Zn-2.3Mg-1.7Cu alloy increased from 212.15 MPa to 248.05 MPa, which is an increase of 16.92%; the elongation (elongation, EL) increased first and then decreased with the increase in Zn content. And the maximum elongation was 8.78% when $x = 5.8$ [11]. The increase in the number of MgZn₂ strengthened phases, and the changes in the shape, number and size of the intercrystalline eutectic phases improved the tensile strength. And the change in elongation was mainly due to the refinement of grain size and the transformation of the dendrite morphology from columnar dendrite to cellular dendrite [12].

2.3.2. Effect of Zn on Softening Behavior of Al-Zn-Mg-Cu Alloys

Zn has an important effect on the softening behavior of Al-Zn-Mg-Cu alloys. At 300 °C, there was a plateau in the static softening curve of the alloy. The increase in Zn content promoted the formation and coarsening of η phases, which also promoted the duration and softening fraction of the plateau decrease (Figure 5a,b). When the deformation temperature increased to 400 °C, the static softening curve was less affected by Zn content (Figure 5c,d) [13]. The effect of Zn content on the dynamic softening behavior is shown in Figure 6. The increase in Zn led to the acceleration of work hardening at the initial deformation stage at 300 °C and the dynamic softening process enhanced with the increase in Zn content. However, at 400 °C, the high supersaturation solid solubility caused by the addition of Zn inhibited the dynamic recovery and recrystallization process, which resulted in a slow-down of the dynamic softening behavior (Figure 6c,d) [14].

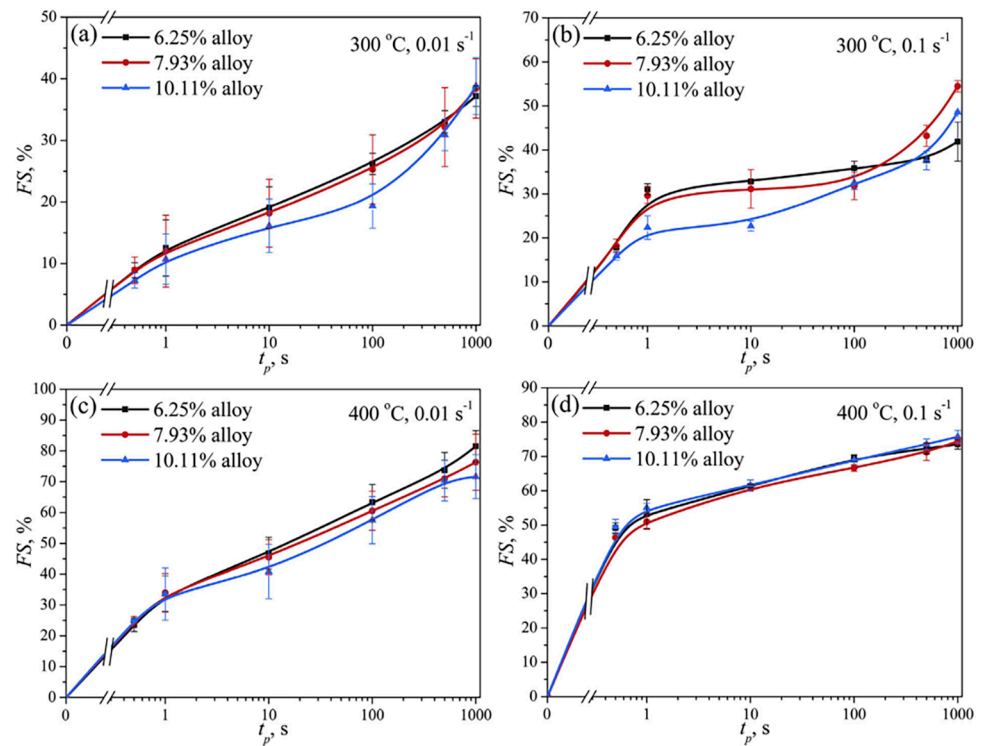


Figure 5. Static softening curves of Al-Zn-Mg-Cu alloy with different Zn contents under two-stage hot compression (a) 300 °C, 0.01 s⁻¹; (b) 300 °C, 0.1 s⁻¹; (c) 400 °C, 0.01 s⁻¹ and (d) 400 °C, 0.1 s⁻¹ (Reprinted with permission from Ref. [13]. 2023 Elsevier).

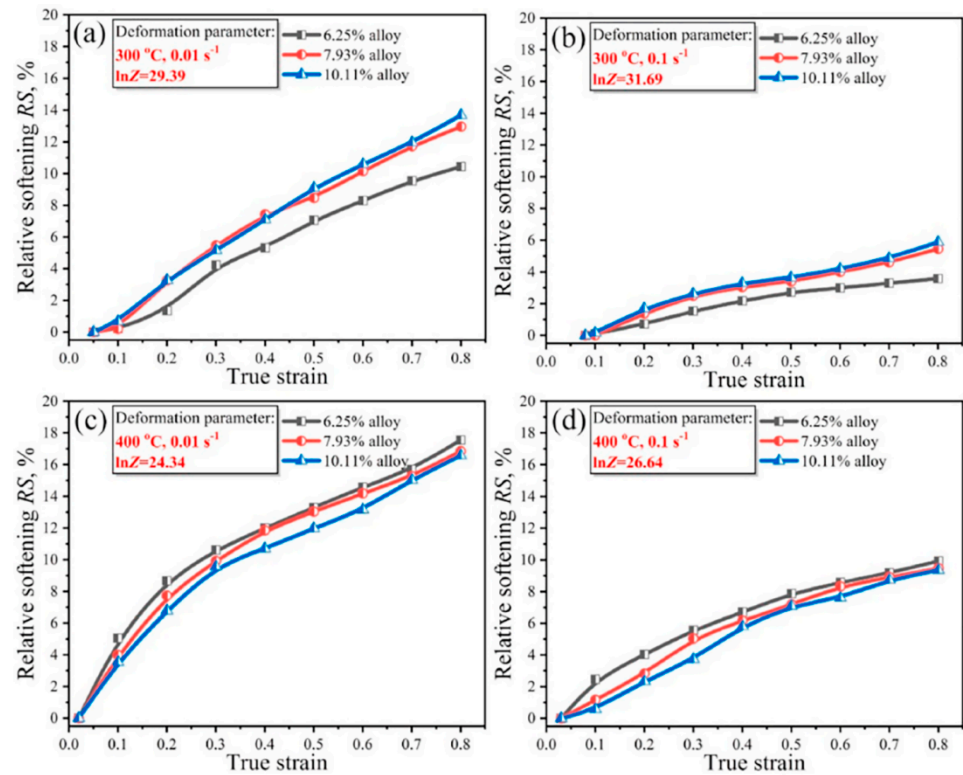


Figure 6. Relative dynamic softening behavior of Al-Zn-Mg-Cu alloys with different Zn contents during continuous compression (a) 300 °C, 0.01 s⁻¹; (b) 300 °C, 0.1 s⁻¹; (c) 400 °C, 0.01 s⁻¹; (d) 400 °C, 0.1 s⁻¹ (Reprinted with permission from Ref. [14]. 2023 Elsevier).

2.3.3. Effect of Zn on Hot-Cracking Sensitivity of Al-Zn-Mg-Cu Alloys

The hot-cracking sensitivity of an Al-Zn-Mg-Cu alloy increases first and then decreases with the increase in Zn content. When the Zn content was 5% (mass fraction) and 11% (mass fraction), the hot-cracking sensitivity was low. And when the Zn content was 9% (mass fraction), the hot-cracking sensitivity was the highest [15]. The thermal cracking sensitivity of the alloy was determined by grain morphology, grain size, thermal shrinkage behavior of the solidification interval and non-equilibrium eutectic content. The increase in Zn content increased the thermal shrinkage of the alloy, which resulted in a larger thermal strain during the solidification process. Although the decrease in grain size helped to reduce the thermal cracking sensitivity of the alloy, the transition from equiaxed spherules to irregular grains reduced the fluidity of the alloy (Figure 7), so the hot-cracking sensitivity of the alloy with 9% Zn content (mass fraction) was the highest. When the content of Zn was further increased to 11% (mass fraction), the grain was refined and transformed from an equiaxed crystal to a fine dendrite and the thermal shrinkage rate increased. But the significant increase in the non-equilibrium eutectic content enabled the alloy to have a better ability to heal the cracks and began to decrease the thermal crack sensitivity.

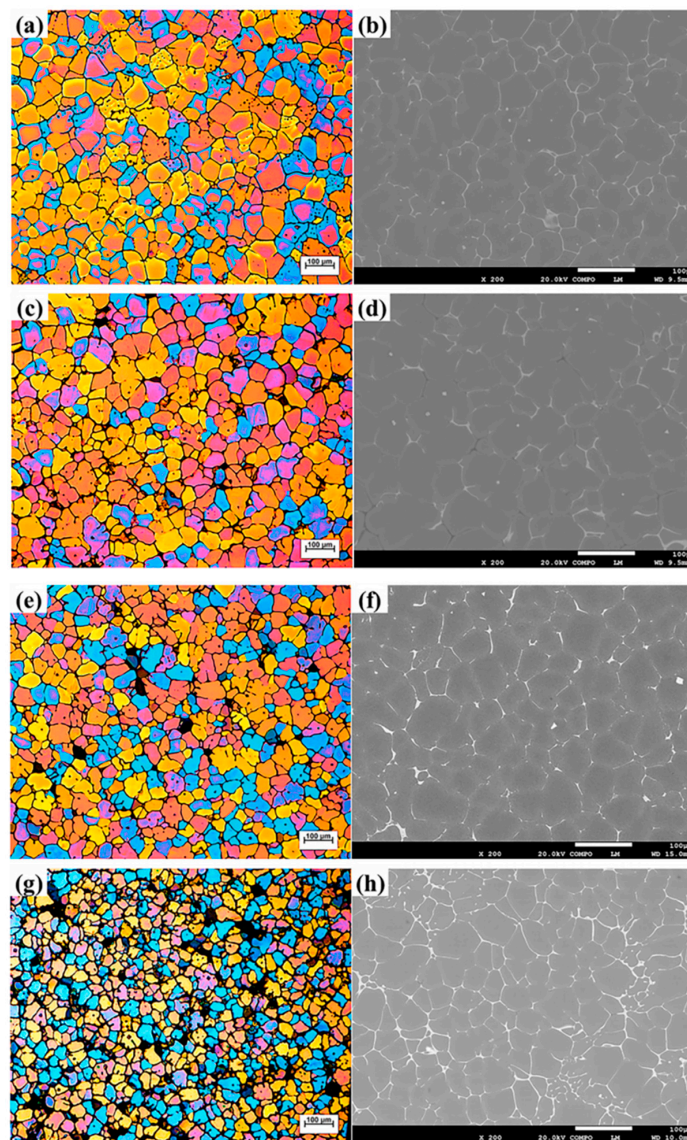


Figure 7. Optical and SEM photos in Al- x Zn- y Mg- z Cu alloys ((a,b): $x = 5$; (c,d): $x = 7$; (e,f): $x = 8$; (g,h): $x = 9$) (Reprinted with permission from Ref. [15]. 2023 Elsevier).

2.3.4. Effect of Zn on Thermal Stability of Al-Zn-Mg-Cu Alloys

BF TEM images and corresponding SAED modes of Al-Mg-Cu alloy with Zn addition after aging at 125 °C for 192 h were shown in the Figure 8. It could be observed from the figure that a large number of small cubic precipitates were evenly distributed in the aluminum matrix and its structure was stable, which could prevent deformation at high temperature. The thermal stability of the alloy was significantly improved [16].

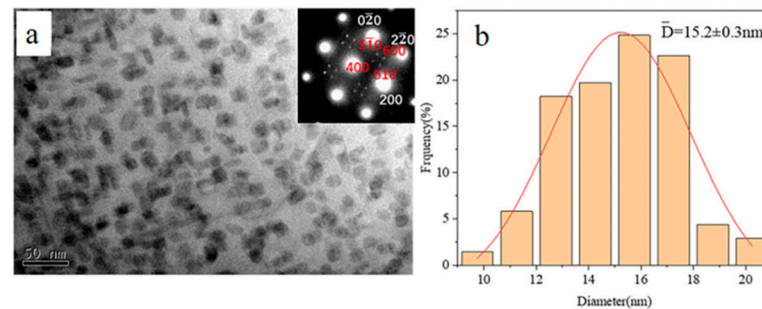


Figure 8. (a): TEM BF micrographs with corresponding SADP pattern taken along $\langle 001 \rangle$ direction, (b): the diameter distribution of precipitates after aging at 125 °C for 192 h (Reprinted with permission from Ref. [16]. 2023 Elsevier).

2.4. Cu/Mg Ratio

2.4.1. The Synergistic Action of Cu and Mg

Mg content was the main factor affecting the strength of over-aged Al-Zn-Mg-Cu alloy. The increase of Cu content could also enhance the strength, but to a lesser extent. In contrast, for spray formed aluminum alloy, the volume fraction of the secondary phase inside the grain was mainly determined by the Mg content and the volume fraction of the secondary phase at the grain boundary was mainly controlled by the Mg + Cu content. After solid solution treatment, coarse grain boundary phase with high Mg content was difficult to enter the single-phase Al region, so the formation of refractory phase in Mg rich (2.65%, mass fraction) aluminum alloy could be promoted by adding Cu element, which was conducive to maintaining the peak strength of the alloy in the over-aging state [8]. In addition, it had been found that compared with non-Cu alloys, the yield strength of Al-4.0Mg-3.0Zn-1.5Cu aluminum alloys with high Cu increased by 80.5%, while the ductility didn't decrease [17]. Therefore, a balance between ductility and strength was expected to be achieved by appropriate adjustment of Cu/Mg ratio.

2.4.2. Effect of Different Cu/Mg Ratio on Al-Zn-Mg-Cu Alloy

The influence of Cu/Mg ratio on Al-Zn-Mg-Cu alloy was mainly reflected in two aspects: one was to affect the coarsening rate in the aging process; the other was to change the size and distribution of precipitated phase. Alloys with a low Cu/Mg ratio had a slow coarsening rate and a high tensile strength. Under T79 aging, Cu/Mg had the highest tensile strength than the lowest 2.5Mg1.5Cu alloy. The alloys with a higher Cu/Mg ratio had coarser Grain boundary precipitates, GBPs) and a wider Precipitate free zone (PFZ) could effectively delay the propagation of microcracks along grain boundaries [18]. With the increase of Cu/Mg ratio, the elongation of Al-Zn-Mg-Cu alloy increased significantly and the fracture morphology changed from the typical brittle fracture to the intergranular mixed fracture or ductile fracture.

2.5. Zn/Mg Ratio

2.5.1. Effect of Zn/Mg Ratio on the Precipitation Sequence and Phase of the Alloy

The Zn/Mg ratio was closely related to the strength and stress corrosion resistance of Al-Zn-Mg-Cu alloy and also affected the precipitation sequence and phase of the alloy. It was generally believed that the precipitation sequence of Al-Zn-Mg-Cu alloy was as follows: SSSS \rightarrow GP region \rightarrow η' phase \rightarrow η' phase (MgZn₂) [19]. With the decrease of Zn/Mg

ratio, T' phase replaces η' phase, and the precipitation sequence changed to SSSS \rightarrow GPI region \rightarrow GPII region \rightarrow intermediate phase T' \rightarrow equilibrium phase $T\text{-Mg}_{32}(\text{Al,Zn})_{49}$ [20].

2.5.2. Effect of Different Zn/Mg Ratio on Al-Zn-Mg-Cu Alloy

The influence of Zn/Mg ratio on mechanical properties of Al-Zn-Mg-Cu alloy was shown in Figure 9. As the Zn/Mg ratio increased from 1.50 to 2.86, the density and strength of precipitated phase in the alloy increased and more solute atoms precipitated at grain boundaries or within grains, which led to a decrease in PFZ width and elongation. When the Zn/Mg ratio further increased from 2.86 to 10.00, the changes in strength and elongation were opposite to those before [21]. In addition, the increase of Zn/Mg ratio could reduce the precipitation of equilibrium η phase during slow quenching, which resulted in the increase of enhanced precipitates after aging treatment, thus reducing the quenching sensitivity of the alloy [22]. For high Zn/Mg ratio alloys, the critical cooling rate without precipitation during the cooling process was about 100 K/s. While for low Zn/Mg ratio alloys, the critical cooling rate was about 1 K/s [23]. Therefore, Al-Zn-Mg-Cu alloys with high Zn/Mg ratio showed higher quenching sensitivity and were more prone to hot cracking.

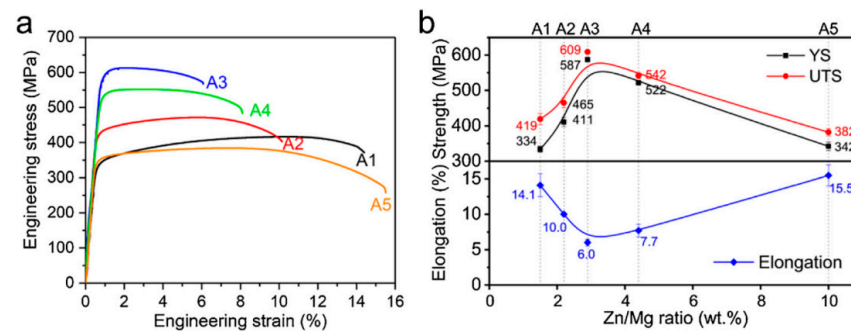


Figure 9. Mechanical properties of peak aged samples: (a) engineering stress–strain curves; (b) strength and elongation values as a function of Zn/Mg ratios (Reprinted with permission from Ref. [21]. 2023 Elsevier).

2.5.3. Effect of Different Zn/Mg Ratio on Corrosion Resistance of Al-Zn-Mg-Cu Alloy

Electrochemical impedance spectroscopy (EIS) revealed the relationship between impedance size, phase Angle, and frequency. Electrochemical impedance spectroscopy (EIS) showed the relationship between electrochemical impedance, phase Angle, medium frequency range and corrosion resistance of electrochemical impedance spectroscopy. With the increase of Zn/Mg ratio, the arc radius and phase Angle of Nyquist curve decreased, which indicated that the corrosion resistance of the alloy decreased [24]. And Al-Zn-Mg-Cu alloy with lower Zn/Mg ratio showed better surface protection and corrosion resistance [25].

2.6. Brief Summary

In conclusion, the influence of alloy elements on the precipitation process can be summarized in the following Table 1. Cu played an important role in the corrosion performance of the alloy, which could adjust the trend of Zn and Mg to decrease the corrosion resistance when the strength and hardness were increased. At the same time, Zn could make the alloy have high plasticity properties, which was expected to achieve a balance between ductility and strength. Therefore, adjusting the proportion between the main elements and finding the threshold between the proportion of elements could effectively solve the contradiction between strength and toughness and corrosion resistance.

Table 1. Effect of alloy elements on the precipitation process.

Alloy Element Content	Dissolving Process
low Zn/Mg ratio	α (supersaturated solid solution) \rightarrow GP region $\rightarrow \eta'$ (MgZn ₂) $\rightarrow \eta$ (MgZn ₂)
high Zn/Mg ratio	α (supersaturated solid solution) \rightarrow GP region $\rightarrow T'$ (Al ₂ Mg ₃ Zn ₂) $\rightarrow T$ (MgZn ₂)
excessive Cu	α (supersaturated solid solution) \rightarrow GP region $\rightarrow \eta'$ (MgZn ₂) $\rightarrow S$ (MgZn ₂)

3. Microalloy Elements

Trace elements in Al-Zn-Mg-Cu alloys include two categories: First is impurity elements, mainly Fe and Si. A small amount of impurity elements inevitably exist in aluminum alloys and with the recycling of recycled aluminum, the content of Fe and Si in the alloys will further increase. The second is alloying elements including Ag, Ni, Ti, etc. Microalloying elements are mainly introduced to refine grain and improve alloy strength.

3.1. Fe, Si

3.1.1. Effect of Fe and Si on the Properties of Al-Zn-Mg-Cu Alloys

Fe and Si were the most common impurity elements in Al-Zn-Mg-Cu alloys and generally formed coarse Al₇Cu₂Fe, Al₃Fe, α -AlFeSi and Mg₂Si phases in the alloys [26,27]. The brittle and hard Al₇Cu₂Fe phase was not coherent with the α (Al) matrix and was easy to crack or separate from the matrix to form voids. It grew up under the loading stress and eventually formed macroscopic cracks, which led to the fracture of the alloy [28].

When Fe content increased from 0.12% (mass fraction) to 0.26% (mass fraction), the tensile strength of the alloy changed little, where the elongation decreased seriously [29]. When Fe content increased from 0.0% (mass fraction) to 0.6% (mass fraction), the fracture toughness decreased from 40 MPa.m^{1/2} to 30 MPa.m^{1/2} [30]. However, the fatigue life of Al-Zn-Mg-Cu alloys could be improved by reasonable control of Fe content. When the strain amplitude was less than 0.5%, the fatigue life of Al-Zn-Mg-Cu alloy with 0.33% (mass fraction) Fe was obviously better than that with 0.01% (mass fraction) Fe [31]. The reason was that fine Fe-rich phase could change the crack propagation path under low strain amplitude and increased the crack propagation resistance, which improved the fatigue life. However, when the volume fraction and size of the Fe-rich phase exceeded a certain critical value, the Fe-rich phase might still become a crack source, which would damage the fatigue property of the alloy.

The Al-4.5Zn-1.5Mg-1.0Cu-0.35Si alloy contained fine and dispersed plate-strip precipitates in the intragranular structure, which was called the GPB-II zone [32]. The GPB-II zone exhibited stronger stability than η' and T' phases under high temperature aging, which significantly improved the alloy strength [33]. After aging at 125 °C, 175 °C and 225 °C, the microhardness and strength of Al-Zn-Mg-Cu alloys containing Si were significantly higher than those without Si.

3.1.2. Effect of Fe and Si on the Recrystallization Process of Al-Zn-Mg-Cu Series Alloys

Fe and Si could change the mechanical properties of Al-Zn-Mg-Cu alloy by influencing the recrystallization process. The change of grain boundary orientation distribution was closely related to recrystallization caused by Particle stimulated nucleation (PSN) of Al₇Cu₂Fe and Mg₂Si [34]. Figure 10 shows the EBSD pattern of the matrix around the coarse intermetallic particles in the longitudinal section of the aging alloy, with the white line showing a low Angle boundary of 1.5° to 15° (LAGBs) and the black line showing a high Angle boundary greater than 15° (HAGBs). The local deformation zones (outlined with yellow dashed lines) of each kind of particles extending from the particle-matrix interface to the neighboring matrix were evidently observed through the EBSD micrographs. With the increase of Fe and Si content, the density of Al₇Cu₂Fe and Mg₂Si increased. It was easier to induce recrystallization and formed recrystallized grains whose orientation was much different from the texture direction of extruded fibers, which contributed to the formation of more high Angle grain boundaries. when the mass fraction of Fe and Si

increased from 0.041% and 0.024% to 0.272% and 0.134%, respectively, Recrystallization resulted in a decrease in the texture of extruded fibers from 56.8% to 53.8% [35], which decreased slightly strength. High angle grain boundaries hindered deformation more seriously and promote intergranular fracture more easily than low Angle grain boundaries. Therefore, with the increase of Fe and Si content, a large number of coarse $\text{Al}_7\text{Cu}_2\text{Fe}$ and Mg_2Si phases and more high Angle grain boundaries would also reduce the elongation.

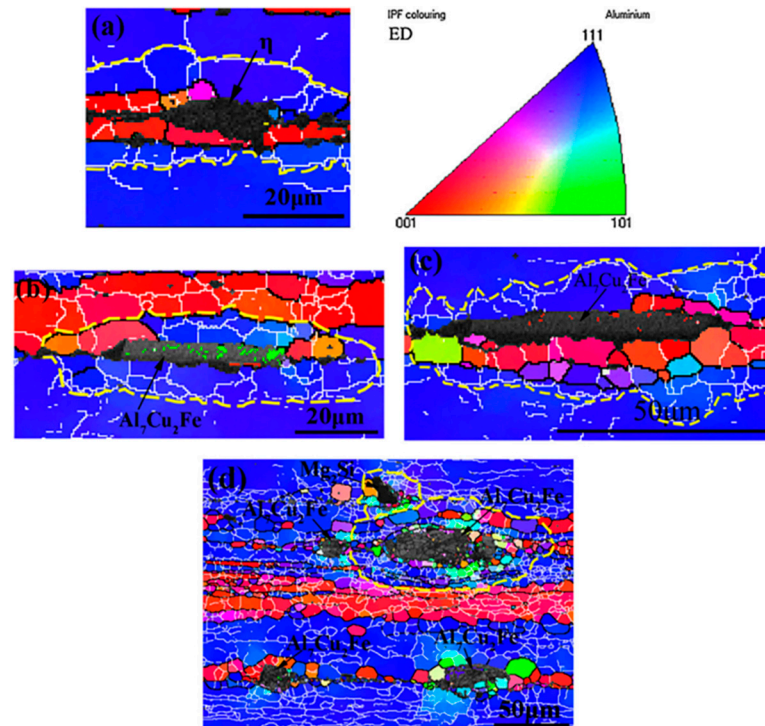


Figure 10. EBSD patterns of the matrix surrounding coarse intermetallic particles in the longitudinal section of aged alloys: (a) η /S in 7055 alloy; (b) $\text{Al}_7\text{Cu}_2\text{Fe}$ in 7055 alloy; (c) $\text{Al}_7\text{Cu}_2\text{Fe}$ larger than $70\ \mu\text{m}$ in 7055 alloy; (d) $\text{Al}_7\text{Cu}_2\text{Fe}$ and Mg_2Si in another 7055 alloy (Reprinted with permission from Ref. [35]. 2023 Elsevier).

3.2. Ag

3.2.1. Effect of Ag on the Hardness and Yield Strength of Al-Zn-Mg-Cu Alloy

Ag could significantly improve the early aging response and the overall aging response of Al-Zn-Mg-Cu alloy [36], which increased the density of fine aggregates. The aggregate density of 7075 alloy after peak aging was $1.2 \times 10^{24}\ \text{m}^{-3}$, which increased to $3.1 \times 10^{24}\ \text{m}^{-3}$ after adding 0.3% Ag. The increase of fine T-phase and η phase density in Ag-containing alloys increased the hardness and yield strength by more than 10% [37].

3.2.2. Effect of Ag on the Corrosion Resistance of Al-Zn-Mg-Cu Alloy

The tensile strength of Al-4.5Zn-1.55Mg-0.12Cu alloy with 0.12% Ag added was 457.6 MPa in 3.5% NaCl solution, and it was 20.5 MPa higher than that without Ag added, which loss elongation little and showed better corrosion resistance to NaCl solution (Figure 11) [38]. On the one hand, Ag atoms were distributed around the grain boundary precipitated phase, which significantly reduced the potential difference between PFZ and GBPs, increased pitting potential, and reduced the sensitivity of the alloy to stress corrosion cracking. On the other hand, the addition of trace Ag could increase the size of precipitated phase and the distance between precipitated phases, which was conducive to the capture of hydrogen atoms in the grain boundary, so as to improve the stress corrosion resistance of the alloy.

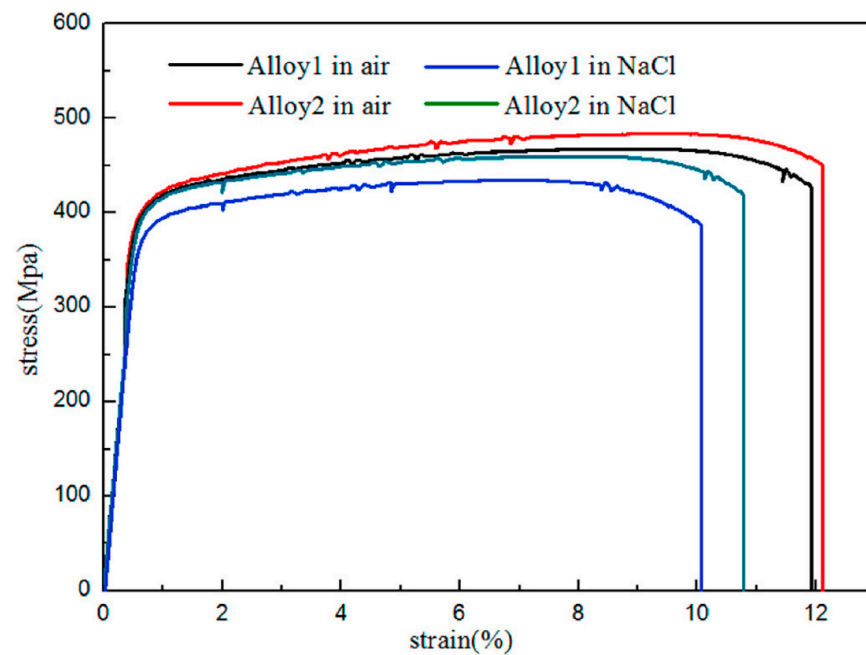


Figure 11. Stress-strain curves of the Al-4.5Zn-1.55Mg-0.12Cu alloys (Alloy 1: without Ag addition; Alloy 2: 0.12 wt.% Ag) (Reprinted with permission from Ref. [38]. 2023 Elsevier).

3.2.3. Effect of Ag on the Fracture of Al-Zn-Mg-Cu Alloy

When Ag was added to Al-Zn-Mg-Cu alloys containing Ge, a small amount of Ag could effectively capture vacancy and reduced vacancy loss near the grain boundary, which effectively reduced the width of PFZ. The joint addition of Ge and Ag made Mg_2Ge particles finer and more evenly distributed, which reduced the degree of stress concentration and further improved the plasticity of the alloy. After air cooling, the fracture changed from brittle intergranular fracture to ductile transgranular fracture (Figure 12) [39].

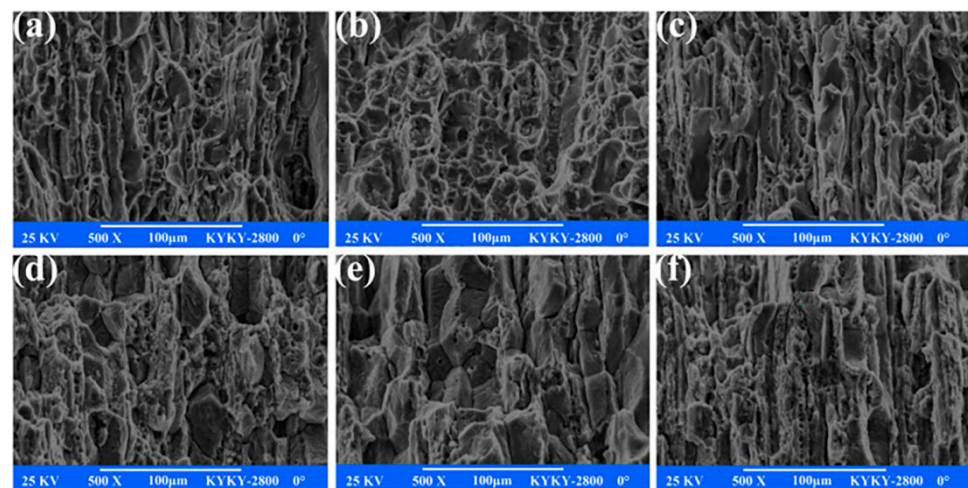


Figure 12. Scanning electron micrographs of fracture surfaces of tensile specimens of water quenching alloys (a–c) and air cooling alloys (d–f): (a,d) Base alloy; (b,e) Add Ge; (c,f) Add (Ge + Ag) (Reprinted with permission from Ref. [39]. 2023 Elsevier).

3.3. Ni

3.3.1. Effect of Ni on the Thermal Cracking Sensitivity of Al-Zn-Mg-Cu Alloy

It had been shown that adding Ni to Al alloy could improve the strength at room temperature or high temperature, which had been confirmed in Al-Zn-Mg-Cu alloy [40]. In the equilibrium phase diagram of Al-Zn-Mg-Cu-Ni alloy, Ni only existed in the form

of (Al + Al₃Ni) eutectic [41]. Generally speaking, the increase of eutectic helped to inhibit the formation of hot cracking of casting alloy, which effectively reduced the hot cracking tendency of alloy.

3.3.2. Effect of Ni on the Strength and Elongation of Al-Zn-Mg-Cu Alloy

In as-cast Al-Zn-Mg-Cu-Ni alloys, the amount of Al₃Ni phase increased with the increase of Ni content. The Al₃Ni phase was formed by $L \rightarrow (\alpha\text{-Al} + \text{Al}_3\text{Ni})$ eutectic reaction at the last stage of solidification. The increase of Al₃Ni phase on the fracture surface meant that there was more residual liquid between the primary α -Al dendrites. In this case, the initial fracture would be filled with residual eutectic liquid, which reduced the possibility of thermal cracking. When the amount of Ni was less than 0.6% (mass fraction), the improvement of grain size and shrinkage defect could improve the tensile strength and elongation at the same time. However, when the Ni content was more than 0.6% (mass fraction), the increase of alloy strength led to the decrease of the elongation (Figure 13). When the Ni content was greater than 1.2% (mass fraction), the alloy had no hot cracking tendency [42]. Therefore, the strength and elongation of Al-Zn-Mg-Cu alloy could be increased by adding appropriate amount of Ni, and the thermal cracking sensitivity could be reduced, so as to improve the service performance of the material.

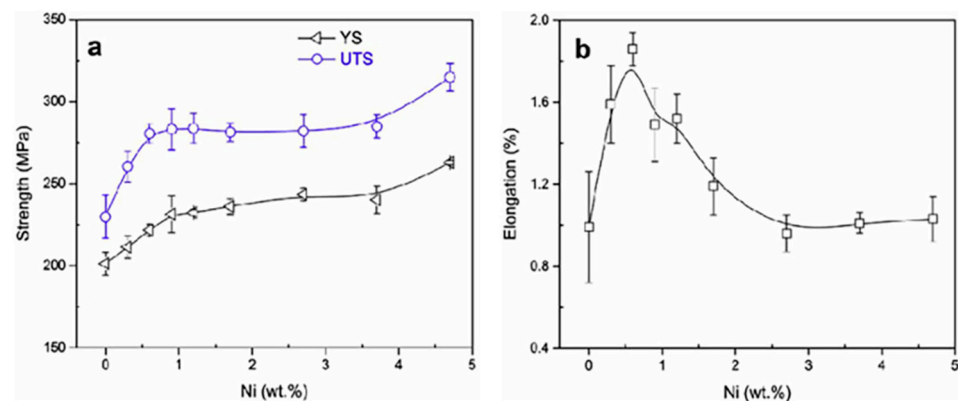


Figure 13. Mechanical properties of the as-cast Al-Zn-Mg-Cu-Ni alloys at room temperature: (a) ultimate tensile strength and yield strength, (b) elongation (Reprinted with permission from Ref. [42]. 2023 Elsevier).

3.4. Ti

3.4.1. Effect of Ti on the Thermal Cracking Sensitivity of Al-Zn-Mg-Cu Alloy

The effects of Ti on Hot tearing sensitivity (HTS) of Al-Zn-Mg-Cu alloys were related to the content of elements. Adding 0.06% (mass fraction) Ti could reduce the hot-cracking sensitivity factor of Al-6Zn-2Mg-2Cu-Ti alloy from 17 (0.00%Ti, mass fraction) to 7 (0.06%Ti, mass fraction). But with further increase of Ti content, the hot-cracking sensitivity factor increased from 7 (0.06%Ti, mass fraction) to 13 (0.24%Ti, mass fraction) [43], which reduced the pouring performance of the alloy.

3.4.2. Effect of Ti on the Strength and Plasticity of Al-Zn-Mg-Cu Alloy

In addition to affecting the hot-cracking sensitivity of the alloy, 0.1% (mass fraction) Ti could also reduce the grain size and the degree of phase agglomeration during the solidification of Al-Zn-Mg-Cu alloy, thus improving the strength and plasticity of the as-cast alloy. The addition of Ti changed the chemical composition of L₁₂ precipitated phase from (Al,Zn)₃Zr to (Al,Zn)₃(Zr,Ti), and the lattice constant decreased from 0.4111 nm to 0.4018 nm. Because the decrease of lattice constant resulted in the lattice mismatch between the precipitated phase and Al matrix, L₁₂ precipitated phase was refined from 18.7 ± 0.4 nm to 14.2 ± 0.4 nm [44]. In addition, the addition of Ti led to the formation of Al₁₈Mg₃Ti₂ metal compound phase during the solid solution process, which played an important role

in the preferential nucleation of η -Mg(Zn,Cu,Al)₂ precipitates in slow-cooling alloys after solid solution treatment [45]. At the same time, the interface between Al₁₈Mg₃Ti₂ phase and Al matrix also provided non-uniform nucleation sites for L1₂ precipitated phase and zinc-rich phase [46].

3.5. Brief Summary

The impurity elements Fe and Si that were controlled in a certain range could not only reduce the appearance of alloy cracks, but also improve the fatigue life and strength of the alloy. Ag played an important role in improving resistance to stress corrosion and solution corrosion. At the same time, the ductility decrease was small. Ti and Ni played a crucial role in improving strength and reducing thermal cracking sensitivity. However, the role of Ag, Ti and Ni also had a threshold and the right amount of addition could play its most effective role. And balance the relationship between mechanical properties.

4. Rare Earth Element

The effects of rare earth elements on Al-Zn-Mg-Cu alloys were similar, which were mainly reflected in the following aspects: on the one hand, the solubility of rare earth elements in aluminum was small and they could form Al₃RE phase with Al. In the solidification process, the Al₃RE phase served as the heterogeneous core of Al matrix, which significantly refined the grains. On the other hand, the dispersing Al₃RE phase was strongly pinned to the dislocation in the process of homogenization and solution aging, which effectively inhibited the recrystallization of the alloy and significantly increased the recrystallization temperature. In addition, rare earth elements could react with H, O, N, C, S, Si, halogen, oxide and other nonmetallic impurities in aluminum melt to form compounds. So this reduced the content of gas content, inclusions and harmful elements in liquid aluminum, which achieved the role of gas removal, slag removal and matrix purification. And it reduced porosity, porosity, slag inclusion and other defects in the ingot, so as to improve the quality of the ingot.

4.1. Sc

4.1.1. Refinement Effect of Sc on Al-Zn-Mg-Cu Alloy

Sc had a very low solid solubility in Al-Zn-Mg-Cu alloy and the presence of Sc led to the formation of primary Al₃Sc phase, which could act as the nucleating particle of Al matrix during solidification and significantly modify the as-cast structure [47]. Al₃Sc phase with different primary morphologies could produce different refining effects, which would affect the mechanical properties of the alloy. Holding at 760 °C for 10 min followed by rapid cooling (at a cooling rate of 100–1000 K/s) could lead to the diversity of primary Al₃Sc phase morphology, and this form of Al-Sc alloy had the best refining effect on Al-Zn-Mg-Cu-Sc-Zr alloy [48].

4.1.2. Effect of Sc on the η' Phase Distribution and Corrosion Resistance of Al-Zn-Mg-Cu Alloys

Sc could not only affect the refining effect of Al-Zn-Mg-Cu alloy during solidification, but also could promote the uniform precipitation of η' phase during aging, which inhibited the coarsening of η' phase and prevented its transition to η phase [49]. Compared with 7055 aluminum alloy without Sc, the addition of 0.25% (mass fraction) of Sc made 7055 aluminum alloy smaller in size and it also made η' phase distribution more uniform, so the alloy had higher hardness, tensile strength, ductility and thermal stability. Sc microalloying could improve the corrosion potential of aluminum alloy, thus improving the corrosion resistance [50]. The addition of trace Sc elements led to an increase in the proportion of grain boundaries in Al-Zn-Mg-Cu alloy, which reduced the amount of precipitated phase per unit grain boundary. Moreover, the discontinuous distribution of precipitated phase along grain boundaries reduced the anodic dissolution rate of precip-

itated phase, which improved the resistance of the alloy to intergranular corrosion and spalling corrosion [51].

4.1.3. Effect of Sc on the Damping Properties of Al-Zn-Mg-Cu Alloy

It had been shown that Sc also affected damping properties of Al-Zn-Mg-Cu alloys. The excellent damping performance of metal was due to the excellent grain boundary sliding ability of its crystal structure, and the fine grain structure always contributed to the improvement of grain boundary sliding ability. Therefore, the damping performance of Al-Zn-Mg-Cu alloy could be improved by refining the grain [52]. For example, reducing grain size, promoting the formation of equiaxed crystals and introducing wetting interface between Al-Zn phase, etc. [53]. 7055 alloy with 0.25% (mass fraction) Sc added was further treated by friction stir, which had fine grain and equiaxed fine crystal structure and showed the best damping performance [54].

4.1.4. Effect of Sc on the Plastic Properties of Al-Zn-Mg-Cu Alloy

The Figure 14 showed a transmission electron micrograph obtained from the measured portion of an Al-Zn-Mg-Cu-0.10Sc-0.10Zr alloy sample at a strain value of 1.10 (corresponding to 200% elongation). It could be observed that a large number of fine $\text{Al}_3\text{Sc}_x\text{Zr}_{1-x}$ particles with Ashby-Brown contrast were evenly distributed inside the particles (black circle) and remained almost constant in size (10–20 nm) during deformation. HRTEM image of the $\text{Al}_3\text{Sc}_x\text{Zr}_{1-x}$ particle was shown in Figure 14c. The $\text{Al}_3\text{Sc}_x\text{Zr}_{1-x}$ particle was spherical with a size of about 15 nm and was completely coherent with the aluminum matrix alloy. These coherent particles strongly fixed dislocations and grain boundaries. As shown by the arrows in Figure 14a,b, they resulted in the controlled growth of microscale grains [55]. Therefore, adding an appropriate amount of Sc to the aluminum alloy could significantly improve the plastic properties of the alloy.

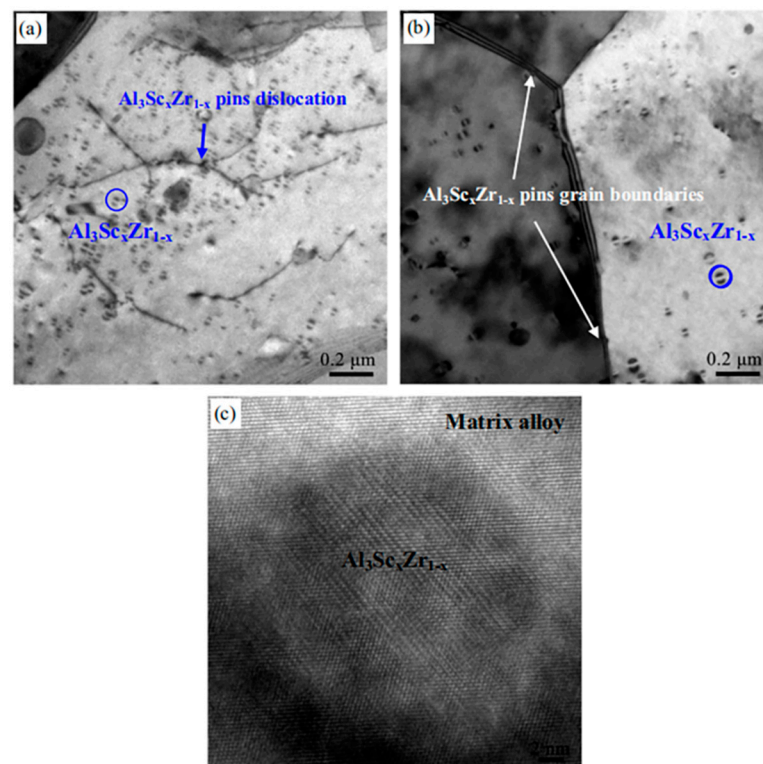


Figure 14. TEM microstructures of specimens deformed after interrupting the tensile test at $\epsilon = 1.10$ (200% elongation) at (a) 450 °C and $5 \times 10^{-3} \text{ s}^{-1}$, (b) 500 °C and $5 \times 10^{-3} \text{ s}^{-1}$ and (c) HRTEM image of the $\text{Al}_3\text{Sc}_x\text{Zr}_{1-x}$ phase in Figure 10b (Reprinted with permission from Ref. [55]. 2023 Elsevier).

4.2. Zr

4.2.1. Refinement Effect of Zr on Al-Zn-Mg-Cu Alloy

Figure 15 shows the effects of mechanical properties of Al-5.8Zn-2.3Mg-1.7Cu alloys at different Zr contents. Adding 0.05% (mass fraction) Zr had no significant effect on grain refinement of Al-Zn-Mg-Cu alloy, but the Brinell hardness reached the maximum. With the increase of Zr content, the grain refinement effect became more obvious. When the addition amount reached 0.20% (mass fraction), the spacing between secondary dendrite arms reached the minimum, and the ultimate tensile strength, yield strength and elongation at room temperature reached the maximum 296.74 MPa, 249.41 MPa and 8.26%, respectively [56].

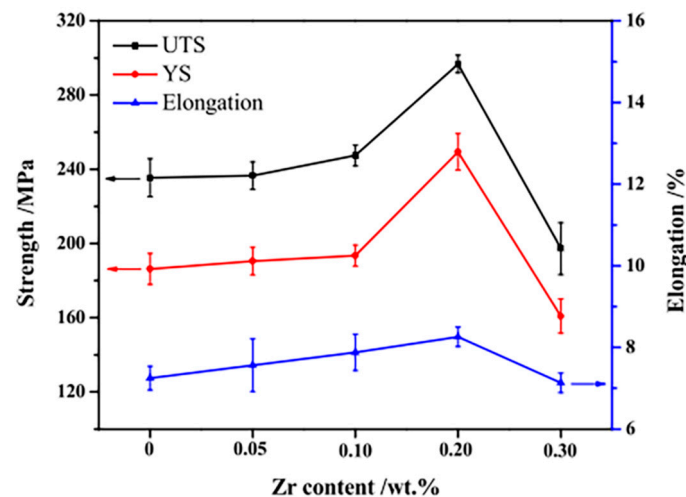


Figure 15. Effect of Zr contents on the mechanical properties of Al-5.8Zn-2.3Mg-1.7Cu alloys with different Zr contents (Reprinted with permission from Ref. [56]. 2023 Elsevier).

4.2.2. Effect of Zr on the Quenching Sensitivity of Al-Zn-Mg-Cu Alloy

When Zr content was within a certain range, fine Al_3Zr dispersion phase could be formed to increase the number of crystal nuclei and refine grains [57]. For Al-Zn-Mg-Cu alloys with high cold-rolling ratio, the coherent interface between Al_3Zr particles and substrate changed to semi-coherent interface after solid solution treatment, which led to non-uniform nucleation of solutes during quenching. So the quenched sensitivity increased that further increased with the cold rolling ratio. In contrast, Alloys with lower cold rolling ratios didn't show any significant quenching sensitivity [58].

4.3. Sc + Zr

4.3.1. Effect of Different Sc + Zr Contents on Al-Zn-Mg-Cu Alloy

The composite addition of trace Sc and Zr resulted in fine-grained strengthening, substructural strengthening, and Orowan mechanism strengthening of $\text{Al}_3(\text{Sc,Zr})$ and Al_3Zr dispersions [59]. By adding 0.07% (mass fraction) Sc and 0.07% (mass fraction) Zr, the strength of the alloy increased about 133 MPa. With the addition of 0.10% (mass fraction) Sc + 0.16% (mass fraction) Zr and 0.22% (mass fraction) Sc + 0.40% (mass fraction) Zr, Al-Zn-Mg-Cu alloy could obtain better recrystallization resistance and thermal stability. And with the increase of Sc and Zr addition, Abundant nano- $\text{Al}_3(\text{Sc,Zr})$ particles could effectively refine dislocations and subgrain boundaries (Figures 16 and 17), which showed good recrystallization resistance and precipitation strengthening effect [60].

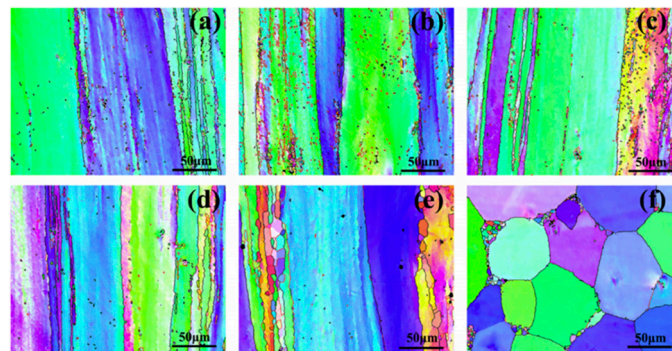


Figure 16. Orientation maps of cold rolled Al-0.3(Sc + Zr) alloy annealed at different temperatures for 1 h: (a) cold rolled; (b) 350 °C; (c) 470 °C; (d) 520 °C; (e) 560 °C; (f) 600 °C (Reprinted with permission from Ref. [60]. 2023 Elsevier).

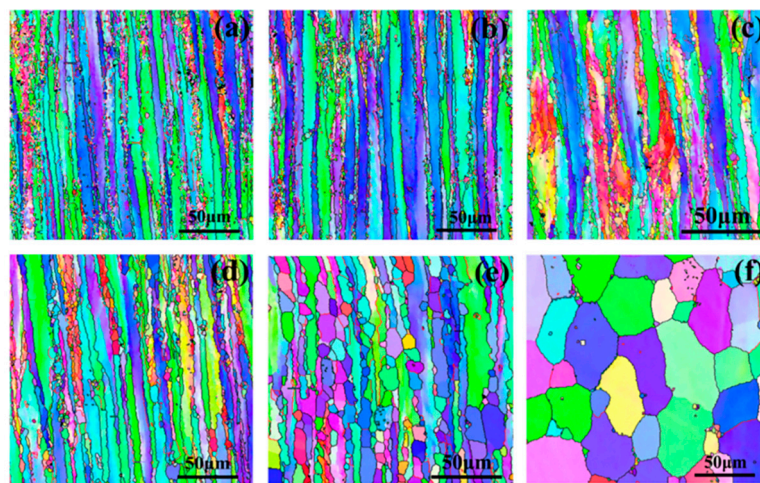


Figure 17. Orientation maps of cold rolled Al-0.6(Sc + Zr) alloy annealed at different temperatures for 1 h: (a) cold rolled; (b) 350 °C; (c) 470 °C; (d) 520 °C; (e) 560 °C; (f) 600 °C (Reprinted with permission from Ref. [60]. 2023 Elsevier).

4.3.2. Effect of Sc + Zr on the Thermal Stability of Al-Zn-Mg-Cu Alloy

The influence of Sc and Zr on the mechanical properties of Al-Zn-Mg-Cu alloys was mainly reflected in Al_3Sc and $\text{Al}_3(\text{Sc},\text{Zr})$. Al_3Sc was the precursor of $\text{Al}_3(\text{Sc},\text{Zr})$ precipitates. Saturated solid solutions containing Sc decomposed at 250 °C, which formed Sc-rich clusters and gradually developed into Al_3Sc crystal nuclei. With the increase of temperature, driven by the chemical potential gradient, Zr atoms began to diffuse over long distances and approached Al_3Sc nuclei. Then they enriched around them to form Zr-rich thin layers, thus forming the $\text{Al}_3(\text{Sc},\text{Zr})$ core/shell structure of Al_3Sc crystal nuclei + Zr-rich shells [61]. The coarsening coefficient of $\text{Al}_3(\text{Sc},\text{Zr})$ precipitates was 3 orders of magnitude smaller than that of Al_3Sc particles, which showed better thermal stability.

4.3.3. Effect of Sc + Zr on the Yield Strength of Al-Zn-Mg-Cu Alloy

However, there was a threshold for the beneficial effect of Sc and Zr combined addition on yield strength. The addition of trace Sc and Zr improved the hardness and yield strength of 7055-T6 alloy by strengthening the grain boundary and $\text{Al}_3(\text{Sc},\text{Zr})$ phase. But in Al-Zn-Mg-Cu alloy with high Cu content, Sc atoms diffused to $\theta\text{-Al}_2\text{Cu}$ phase, which promoted the formation of $w\text{-AlCuSc}$ phase [62]. When the total mass fraction of Sc and Zr exceeded 0.45% (mass fraction), large w phase and coarse primary $\text{Al}_3(\text{Sc},\text{Zr})$ phase were formed, leading to the degradation of mechanical properties of the alloy (Table 2) [63].

Table 2. Tensile properties of 7055-*x*Zr-*y*Sc alloy after rolling and T6 aging (Reprinted with permission from Ref. [63]. 2023 Elsevier).

7055- <i>x</i> Zr- <i>y</i> Sc	Sc + Zr/wt.%	YS/Mpa	UTS/Mpa	EL/%
7055	0.16	577 ± 2	654 ± 2	12.8 ± 0.4
7055-0.2Sc	0.36	609 ± 2	649 ± 3	13 ± 0.5
7055-0.25Sc	0.41	600 ± 2	679 ± 2	14.3 ± 0.5
7055-0.14Zr-0.15Sc	0.45	602 ± 3	657 ± 4	13.7 ± 0.8
7055-0.14Zr-0.2Sc	0.5	593 ± 3	635 ± 5	10.3 ± 0.6
7055-0.24Zr-0.15Sc	0.55	580 ± 2	616 ± 3	7.3 ± 0.3

Note: (YS: Yield strength, UTS: Ultimate tensile strength, EL: Elongation).

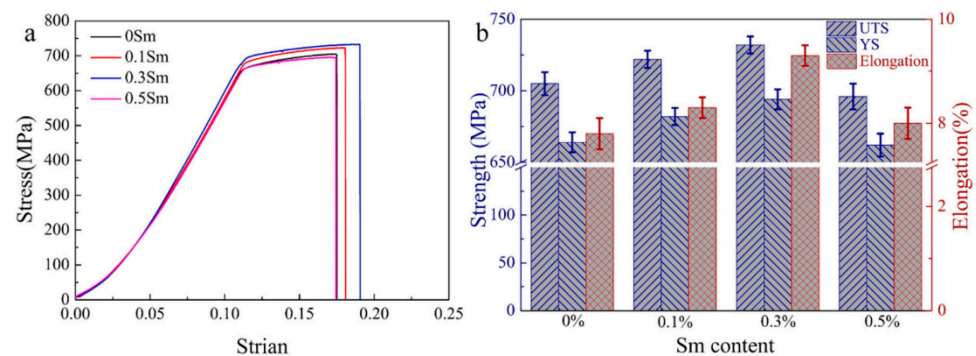
4.4. Sm

4.4.1. Effect of Sm on the Peak Hardness of Al-Zn-Mg-Cu Alloy

Sm could effectively reduce the distance between secondary dendrite arms and was a good thinning element of aluminum alloy. The addition of Sm to Al-Cu alloy could refine the Al₂Cu phase in the alloy and promote its precipitation during aging [64]. The as-cast microstructure of Al-Zn-Mg-Cu-Zr alloy containing Sm mainly included η-(Mg(Zn,Cu,Al)₂) phases, Al₁₀Cu₇Sm₂ phases and Fe-rich phases, and there were also fine η phases and acicular θ(Al₂Cu) phases distributed in the grain [65]. The addition of Sm made the peak aging reach earlier and prolonged the peak aging time. With the increase of Sm content, the peak hardness of the alloy increased first and then decreased, and the maximum peak aging hardness was obtained at 0.3%Sm (mass fraction) [66].

4.4.2. Effect of Sm on the Yield Strength and Elongation of Al-Zn-Mg-Cu Alloy

The effect of Sm content on the ultimate tensile strength, yield strength and elongation of Al-Zn-Mg-Cu alloy at room temperature was similar, which firstly increased and then decreased. When the mass fraction of Sm reached 0.3%, the strengthening effect was the best, and the tensile strength, yield strength and elongation were 732 MPa, 694 MPa and 9.3%, respectively. Compared with unmodified alloy, they were improved by 3.8%, 4.5% and 19%, respectively (Figure 18) [67].

**Figure 18.** Tensile properties of the Al-Zn-Mg-Cu alloys with different Sm contents: (a) stress-strain curves, (b) relationship of ultimate tensile strength, yield strength and elongation with Sm contents (Reprinted with permission from Ref. [67]. 2023 Elsevier).

4.5. Er

In Zr-containing Al-Zn-Mg-Cu alloys, Er and Zr could form dispersed Al₃(Er,Zr) phases [68]. Al₃(Er,Zr) phase could not only serve as the strengthening phase of matrix, but also nailed grain boundaries to inhibit the migration of low-angle grain boundaries to high-angle grain boundaries [69]. η phases tended to preferentially gather at the high Angle grain boundaries with higher energy, but the high Angle grain boundaries with abundant η phases were prone to anodic dissolution, which provided favorable channels for crack propagation [70]. Therefore, the addition of Er could preserve more low Angle grain boundaries, thus improving the corrosion resistance of the alloy. When the Er mass

fraction increases from 0% (mass fraction) to 0.10% (mass fraction), the hardness and yield strength of the alloy increased by 25.4 HV and 70 MPa, respectively, and the intergranular corrosion depth decreased by 65% [71].

4.6. La

In Al-Zn-Mg-Cu alloys, Al-Ti-B was the most commonly used refiner. When La was added to aluminum alloys containing Al-Ti-B, La mainly existed in the form of $Ti_2Al_{20}La$ phase [72]. $Ti_2Al_{20}La$ phase was a non-thermodynamically stable phase [73], which could release rare earth elements. The rare earth could combine with TiB_2 particles to form “rare earth film”, which reduced the free energy of TiB_2 phase and hindered the aggregation and growth of TiB_2 phase, thus maintaining the long-term refining ability of Al-Ti-B. In addition, La atoms significantly promoted the nucleation and motion of dislocation and could promote the twinning deformation at the crack tip, thus inhibiting brittle propagation. Moreover, high concentration of La atoms was conducive to promoting twin deformation and improving the plastic deformation ability of grain boundaries [74]. When 0.3% (mass fraction) of La was added into Al-6.7Zn-2.6Mg-2.0Cu-0.1Zr alloy, the tensile strength and yield strength were 583 MPa and 559 MPa, respectively, which were 18 MPa and 19 MPa higher than those without La modification [75].

4.7. Ce

4.7.1. The Effect of Ce on the Second Phase in Al-Zn-Mg-Cu Alloy

Al-Zn-Mg-Cu alloys without Ce had a high degree of Cu saturation, which would provide more Cu atoms to form Al_2CuMg phase, which resulted in a more stable Al_2CuMg particles. After adding 0.12%Ce (mass fraction), the stable AlCuCe phase could trap a large number of Cu atoms, effectively inhibit the further formation of Al_2CuMg phase [76], and it facilitated the dissolution of homogenization process. When Ce content increased to 0.3% (mass fraction), Al_4Ce phase appeared in the alloy [75]. In the process of solution treatment, fine Al_4Ce phase could nail the grain boundary, inhibit recrystallization and refine the structure.

4.7.2. The Effect of Ce on the Corrosion Resistance on Al-Zn-Mg-Cu Alloy

In addition, adding Ce to Al-Zn-Mg aluminum alloy could significantly prolong the stress corrosion cracking time and reduce the stress corrosion sensitivity. When 0.04% (mass fraction) Ce was added to Al-Zn-Mg aluminum alloy, Ce atoms and Al atoms could be oxidized simultaneously to form rare-aluminum composite oxide film (Al_2O_3 , Ce_2O_3 and $(Al,Ce)_2O_3$) [77], which improved the resistance of passivation film, significantly reduced the self-corrosion current density, and significantly improved the corrosion resistance of the alloy [78].

4.8. Y

4.8.1. Effect of Y on the Effect of Al-Zn-Mg-Cu Alloy Refinement and Dislocation Density

The addition of 7.5% (mass fraction) Y in aluminum alloy could greatly improve the degree of grain refinement and dislocation density. And the formation of $\beta-Al_3Y$ intermetallic phases at grain boundaries could not only promote nucleation, but also prevented grain growth, for which Al-7.5% (mass fraction) Y alloy could maintain fine grains in annealed state [79]. In 6063 aluminum alloy, the combined addition of rare earth Y and Al-Ti-B also played a role in reducing the grain size [80].

4.8.2. Effect of the Phase of the Y on the Al-Zn-Mg-Cu Alloy

In Al-Zn-Mg-Cu alloys, adding Y element alone could refine dendrite substructure and increase the proportion of equiaxed crystals. The combined addition of Zr, Ti and Y could simultaneously refine the grain and dendrite substructure, and the tensile strength could reach about 700 MPa [81]. The synergistic strengthening of rare earth Y with transition elements Zr and Ti might be related to the formation of Al_8Cu_4Y and $Al_3(Zr,Y)$ phases in

the nanonetwork structure. The ideal tensile strength of $\text{Al}_8\text{Cu}_4\text{Y}$ phase in (100) [001] slip system was 15.4 GPa [82], and it had good mechanical properties and thermal stability. The nanocrystalline $\text{Al}_8\text{Cu}_4\text{Y}$ phase was a more ideal existence form than the conventional $\text{Al}_8\text{Cu}_4\text{Y}$ phase. The strengthening of Al-Zn-Mg-Cu alloys had a wider application prospect.

4.9. Ta

The growth limiting factor Q value of Ta in aluminum alloy was 10.5 K. It had been shown that the larger the Q value is, the more obvious the grain refinement effect is [83]. And Ta and Al had higher chemical activity and could form Al_3Ta phase in situ. The Al_3Ta phase with Al had small mismatch, which had been proven to be an efficient grain refiner for additive manufacturing [84].

Al-Zn-Mg-Cu alloy was prepared by laser powder bed melting (3D printing). The addition of 2% (mass fraction) Ta replaced Al atoms in the nano- Al_2Cu phase, and Al_3Ta and AlTaCu nano-phases were formed by in-situ reaction, which prevented coarsening during solidification. These nanophases could inhibit hot cracking, refine and strengthen the alloy, and accelerate the aging process by hetero-nucleation or by hindering the oriented epitaxy growth of grains, thus increasing the ultimate tensile strength from 103 ± 21 MPa to 401 ± 11 MPa (Figure 19b). The aluminum alloy with Ta had a high Angle grain boundary, which could be used as a source of dislocation in the deformation process [85]. Therefore, the grain boundary surface of the alloy melted by laser powder bed had a high density of dislocation sources, which was conducive to deformation and thus to enhancing ductility. The addition of Ta transformed the fracture morphology from brittle intergranular fracture (Figure 19a) to ductile fracture (Figure 19c), and the elongation increased from $0.8 \pm 0.4\%$ to $5.1 \pm 0.6\%$. In addition, the discontinuous ultrafine grains and grain boundaries could inhibit the expansion of corrosion path, reduce the corrosion sensitivity of grain boundaries, and improve the Cl^- corrosion resistance of Al-Zn-Mg-Cu alloy [86].

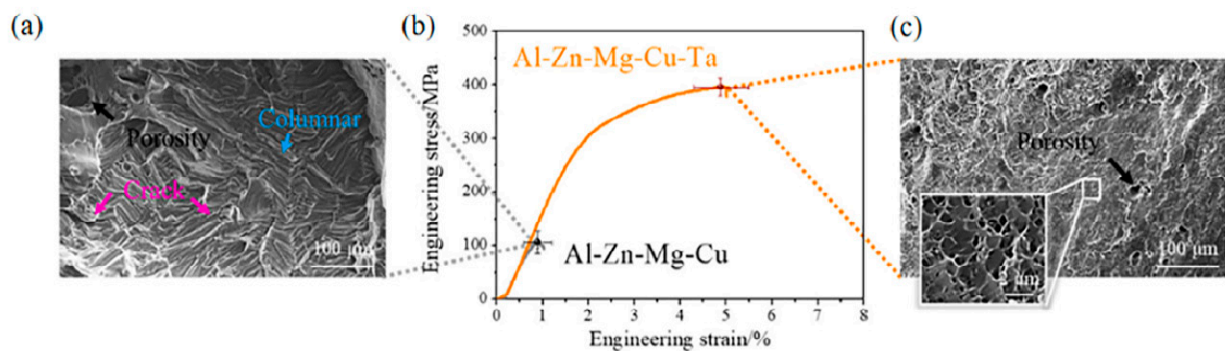


Figure 19. Tensile properties and fracture morphologies of the laser powder bed fusion-fabricated alloys: (a) fracture of Al-Zn-Mg-Cu, (b) stress-strain relations, and (c) fracture of Al-Zn-Mg-Cu-Ta [86].

4.10. Brief Summary

In summary, the rare-earth phases are summarized as follows (Table 3). Sc played an important role in refining grain, improving toughness and corrosion resistance [87,88]. However, due to its high cost, it was not conducive to widespread industrial application and it was necessary to achieve the same effect by low-cost rare earth elements or composite addition. For example, the combined addition of Sc and Zr could not only promote precipitation strengthening, but also improve thermal stability. Other rare earth elements Sm, Er, La, Ce, Y and Ta all played different roles in refining grains. Among them, Er and Ce could greatly improve the corrosion resistance of the alloy. Sm and La played a role in improving the tensile strength. It is important to clarify the main functions and effects of each rare earth element. Compound addition of rare earth elements that reduced cost and balanced performance were urgent problems in the development of alloys.

Table 3. Rare-earth phase in the aluminum alloy.

Rare Earth Element	Rare Earth Phase	Crystal Structure
Sc	Al ₃ Sc	FCC
Sm	Al ₁₀ Cu ₇ Sm ₂	Hexagonal structure
Er	Al ₈ Cu ₄ Er	Hexagonal structure
Ce	Al ₄ Ce	FCC
La	Al ₁₁ La ₃	FCC
Y	Al ₈ Cu ₄ Y	Hexagonal structure
Ta	Al ₃ Ta	FCC

5. Forecast

The effect of alloying on the microstructure and properties of Al-Zn-Mg-Cu alloy was reviewed. For the purpose of corrosion resistance, the ratio of Zn/Mg should be appropriately reduced to improve the corrosion resistance, and the content of Cu should be controlled to avoid the potential difference between grain boundary and Al matrix to cause the corrosion of precipitated phase. In order to achieve comprehensive energy, the iron-rich phase should be made as small as possible to reduce the adverse effects of impurity elements such as Fe and Si on plasticity and fracture toughness. By adding Sc, Zr and other rare earth elements, solution strengthening, aging strengthening and fine crystal strengthening should be introduced to improve the strength and toughness of the alloy. In addition, considering the machining properties of Al-Zn-Mg-Cu alloy, the quenching sensitivity of the alloy should be reduced by adding an appropriate amount of Ge element and the hot cracking tendency should be reduced by adding Ni element. According to the research status and existing problems of alloying Al-Zn-Mg-Cu alloy, the future research directions are as follows:

(1). Optimize the content of main alloy elements and control the content ratio of different main alloys, especially the content ratio of Zn/Mg to Zn/Cu. The influence mechanism of the main alloying elements on the microstructure and properties of Al-Zn-Mg-Cu alloy is studied deeply, and the action threshold of the main alloying elements is defined.

(2). Reduce the content of impurity elements to reduce the influence of impurity elements on the microstructure and properties of the alloy. The strong toughness and corrosion resistance of the alloy can be improved by adding microalloying elements as needed, especially by adjusting the content of rare earth elements and adding compound rare earth elements. The effects of precipitated phase content and distribution on the properties of Al-Zn-Mg-Cu alloys are analyzed and studied to improve the comprehensive mechanical properties of Al-Zn-Mg-Cu alloys.

(3). Combining the effects of main alloying elements and trace alloying elements, the optimal alloying ratio of elements is analyzed through experimental tests, and the mechanism is explored to further optimize the microstructure and mechanical properties of the alloy.

Author Contributions: Investigation, Data curation, and Writing—original draft, J.W.; Project administration, Investigation, and Writing—revised, F.L. All authors have read and agreed to the published version of the manuscript.

Funding: This research was funded by the Hunan Provincial Natural Science Foundation of China (No. 2021JJ30672), Science and Technology Project of Education Department of Hunan Province (No. 22A0100), College Students' innovation and entrepreneurship training program of Xiangtan University.

Institutional Review Board Statement: Not applicable.

Informed Consent Statement: Not applicable.

Data Availability Statement: Not applicable.

Acknowledgments: The authors gratefully acknowledge the support provided by Materials Intelligent Design College Students' Innovation and Entrepreneurship Education Center, Xiangtan University, Xiangtan, Hunan, China.

Conflicts of Interest: The authors declare no conflict of interest.

References

1. Hsiao, T.-J.; Chiu, P.-H.; Tai, C.-L.; Tsao, T.-C.; Tseng, C.-Y.; Lin, Y.-X.; Chen, H.-R.; Chung, T.-F.; Chen, C.-Y.; Wang, S.-H. Effect of Cu Additions on the Evolution of Eta-prime Precipitates in Aged AA 7075 Al-Mg-Zn-Cu Alloys. *Metals* **2022**, *12*, 2120. [[CrossRef](#)]
2. Jiao, H.; Chen, K.; Chen, S.; Yang, Z.; Xie, P.; Chen, S. Effect of Cu on the Fracture and Exfoliation Corrosion Behavior of Al-Zn-Mg-xCu Alloy. *Metals* **2018**, *8*, 1048. [[CrossRef](#)]
3. Chinh, N.; Lendvai, J.; Ping, D.; Hono, K. The effect of Cu on mechanical and precipitation properties of Al-Zn-Mg alloys. *J. Alloys Compd.* **2004**, *378*, 52–60. [[CrossRef](#)]
4. Mondal, C.; Mukhopadhyay, A. On the nature of T(Al₂Mg₃Zn₃) and S(Al₂CuMg) phases present in as-cast and annealed 7055 aluminum alloy. *Mater. Sci. Eng. A* **2005**, *391*, 367–376. [[CrossRef](#)]
5. Dong, P.; Chen, S.; Chen, K. Effects of Cu content on microstructure and properties of super-high-strength Al-9.3Zn-2.4Mg-xCu-Zr alloy. *J. Alloys Compd.* **2019**, *788*, 329–337. [[CrossRef](#)]
6. Zhao, Y.; Li, H.; Liu, Y.; Huang, Y. The microstructures and mechanical properties of a highly alloyed Al-Zn-Mg-Cu alloy: The role of Cu concentration. *J. Mater. Res. Technol.* **2022**, *18*, 122–137. [[CrossRef](#)]
7. Huang, R.; Li, M.; Yang, H.; Lu, S.; Zuo, H.; Zheng, S.; Duan, Y.; Yuan, X. Effects of Mg contents on microstructures and second phases of as-cast Al-Mg-Zn-Cu alloys. *J. Mater. Sci. Technol.* **2022**, *21*, 2105–2117. [[CrossRef](#)]
8. Li, H.; Cao, F.; Guo, S.; Jia, Y.; Zhang, D.; Liu, Z.; Wang, P.; Scudino, S.; Sun, J. Effects of Mg and Cu on microstructures and properties of spray-deposited Al-Zn-Mg-Cu alloys. *J. Alloys Compd.* **2017**, *719*, 89–96. [[CrossRef](#)]
9. Shu, W.; Hou, L.; Zhang, C.; Zhang, F.; Liu, J.; Zhuang, L.; Zhang, J. Tailored Mg and Cu contents affecting the microstructures and mechanical properties of high-strength Al-Mg-Zn-Cu alloys. *Mater. Sci. Eng. A* **2016**, *657*, 269–283. [[CrossRef](#)]
10. Tang, J.; Liu, M.; Bo, G.; Jiang, F.; Luo, C.; Teng, J.; Fu, D.; Zhang, H. Unraveling precipitation evolution and strengthening function of the Al-Zn-Mg-Cu alloys with various Zn contents: Multiple experiments and integrated internal-state-variable modeling. *J. Mater. Sci. Technol.* **2022**, *116*, 130–150. [[CrossRef](#)]
11. Tan, P.; Sui, Y.; Jin, H.; Zhu, S.; Jiang, Y.; Han, L. Effect of Zn content on the microstructure and mechanical properties of as-cast Al-Mg-Zn-Cu alloy with medium Zn content. *J. Mater. Res. Technol.* **2022**, *18*, 2620–2630. [[CrossRef](#)]
12. Curle, U.; Cornish, L.; Govender, G. Predicting yield strengths of Al-Zn-Mg-Cu-(Zr) aluminium alloys based on alloy composition or hardness. *Mater. Des.* **2016**, *99*, 211–218. [[CrossRef](#)]
13. Tang, J.; Zhang, H.; Teng, J.; Fu, D.; Jiang, F. Effect of Zn content on the static softening behavior and kinetics of Al-Mg-Zn-Cu alloys during double-stage hot deformation. *J. Alloys Compd.* **2019**, *806*, 1081–1096. [[CrossRef](#)]
14. Tang, J.; Wang, J.; Teng, J.; Wang, G.; Fu, D.; Zhang, H.; Jiang, F. Effect of Zn content on the dynamic softening of Al-Mg-Zn-Cu alloys during hot compression deformation. *Vacuum* **2021**, *184*, 109941. [[CrossRef](#)]
15. Xu, Y.; Zhang, Z.; Gao, Z.; Bai, Y.; Zhao, P.; Mao, W. Effect of main elements (Zn-Mg and Cu) on the microstructure, castability and mechanical properties of 7xxx series aluminum alloys with Zr and Sc. *Mater. Charact.* **2021**, *182*, 111559. [[CrossRef](#)]
16. Mao, J.; Wen, S.; Liang, S.; Wu, X.; Wei, W.; Huang, H.; Gao, K.; Nie, Z. Precipitation behaviors and thermal stability of Al-3.5Mg-1.0Cu alloy with co-addition of Zn and Si. *J. Alloys Compd.* **2023**, *946*, 169401. [[CrossRef](#)]
17. Zhang, Z.; Li, Y.; Li, H.; Zhang, D.; Zhang, J. Effect of high Cu concentration on the mechanical property and precipitation behavior of Al-Mg-Zn-(Cu) crossover alloys. *J. Mater. Sci. Technol.* **2022**, *20*, 4585–4596. [[CrossRef](#)]
18. Wei, S.; Wang, R.; Zhang, H.; Xu, C.; Wu, Y.; Feng, Y. Influence of Cu/Mg ratio on microstructure and mechanical properties of Al-Mg-Zn-Cu alloys. *J. Mater. Sci.* **2021**, *56*, 3472–3487. [[CrossRef](#)]
19. Chung, T.-F.; Yang, Y.-L.; Huang, B.-M.; Shi, Z.; Lin, J.; Ohmura, T.; Yang, J.-R. Transmission electron microscopy investigation of separated nucleation and in-situ nucleation in AA7050 aluminium alloy. *Acta Mater.* **2018**, *149*, 377–387. [[CrossRef](#)]
20. Hou, S.; Liu, P.; Zhang, D.; Zhang, J.; Zhuang, L. Precipitation hardening behavior and microstructure evolution of Al-5.1 Mg-0.15Cu alloy with 3.0Zn (wt %) addition. *J. Mater. Sci.* **2018**, *53*, 3846–3861. [[CrossRef](#)]
21. Zou, Y.; Wu, X.; Tang, S.; Zhu, Q.; Song, H.; Guo, M.; Cao, L. Investigation on microstructure and mechanical properties of Al-Zn-Mg-Cu alloys with various Zn/Mg ratios. *J. Mater. Sci. Technol.* **2021**, *85*, 106–117. [[CrossRef](#)]
22. Liu, S.; Xu, G.; Li, Y.; Huang, L.; Tang, L.; Peng, X. The Influence of the Zn/Mg ratio on the quench sensitivity of Al-Zn-Mg-Cu alloys. *J. Mater. Eng. Perform.* **2020**, *29*, 5787. [[CrossRef](#)]
23. Graf, G.; Spoerk-Erdely, P.; Staron, P.; Stark, A.; Martin, F.M.; Clemens, H.; Klein, T. Quench rate sensitivity of age-hardenable Al-Zn-Mg-Cu alloys with respect to the Zn/Mg ratio: An in situ SAXS and HEXRD study. *Acta Mater.* **2022**, *227*, 117727. [[CrossRef](#)]
24. Zhang, C.; Lv, P.; Cai, J.; Zhang, Y.; Xia, H.; Guan, Q. Enhanced corrosion property of W-Al coatings fabricated on aluminum using surface alloying under high-current pulsed electron beam. *J. Alloys Compd.* **2017**, *723*, 258–265. [[CrossRef](#)]
25. Li, C.; Xu, X.; Chen, H.; Tabie, V.; Cai, J.; Liu, Y.; Liu, Z.; Peng, C.-T. Effect of Zn/Mg Ratio on Microstructure and Properties of Cold Extruded Al-xZn-2.4Mg-0.84Cu-0.2Zr-0.25Ti Aluminum Alloy. *J. Mater. Eng. Perform.* **2020**, *29*, 5787–5795. [[CrossRef](#)]

26. Li, X.; Starink, M. Identification and analysis of intermetallic phases in overaged Zr-containing and Cr-containing Al-Mg-Zn-Cu alloys. *J. Alloys Compd.* **2011**, *509*, 471–476. [[CrossRef](#)]
27. Lv, X.; Guo, E.; Li, Z.; Wang, G. Research on microstructure in as-cast 7A55 aluminum alloy and its evolution during homogenization. *Rare Met.* **2011**, *30*, 664–668. [[CrossRef](#)]
28. Morgenevner, T.; Starink, M.; Sinclair, I. Evolution of voids during ductile crack propagation in an aluminium alloy sheet toughness test studied by synchrotron radiation computed tomography. *Acta Mater.* **2008**, *56*, 1671–1679. [[CrossRef](#)]
29. Vratnica, M.; Pluvinaige, G.; Jodin, P.; Cvijović, Z.; Rakin, M.; Burzić, Z. Influence of notch radius and microstructure on the fracture behavior of Al-Mg-Zn-Cu alloys of different purity. *Mater. Des.* **2010**, *31*, 1790–1798. [[CrossRef](#)]
30. Ohira, T.; Kishi, T. Effect of iron content on fracture toughness and cracking processes in high strength Al-Zn-Mg-Cu alloy. *Mater. Sci. Eng.* **1986**, *78*, 9–19. [[CrossRef](#)]
31. Hu, K.; Lin, C.; Xia, S.; Zheng, C.; Lin, B. Effect of Fe content on low cycle fatigue behavior of squeeze cast Al-Zn-Mg-Cu alloys. *Mater. Charact.* **2020**, *170*, 110680. [[CrossRef](#)]
32. Kovarik, L.; Court, S.; Fraser, H.; Mills, M. GPB zones and composite GPB/GPBII zones in Al-Cu-Mg alloys. *Acta Mater.* **2008**, *56*, 4804–4815. [[CrossRef](#)]
33. Guo, K.; Liang, S.; Wen, S.; Wei, W.; Hu, J.; Wu, X.; Gao, K.; Huang, H.; Nie, Z. GPB-II zone in Si microalloyed Al-Mg-Zn-Cu alloy and its strengthening effect. *Mater. Sci. Eng. A* **2022**, *852*, 143721. [[CrossRef](#)]
34. Zeng, X.H.; Xue, P.; Wu, L.H.; Ni, D.R.; Xiao, B.L.; Wang, K.S.; Ma, Z.Y. Microstructural evolution of aluminum alloy during friction stir welding under different tool rotation rates and cooling conditions. *J. Mater. Sci. Technol.* **2019**, *35*, 972. [[CrossRef](#)]
35. She, H.; Shu, D.; Dong, A.; Wang, J.; Sun, B.; Lai, H. Relationship of particle stimulated nucleation, recrystallization and mechanical properties responding to Fe and Si contents in hot-extruded 7055 aluminum alloys. *J. Mater. Sci. Technol.* **2019**, *35*, 2570–2581. [[CrossRef](#)]
36. Zhu, Q.; Cao, L.; Wu, X.; Zou, Y.; Couper, M.J. Effect of Ag on age-hardening response of Al-Zn-Mg-Cu alloys. *Mater. Sci. Eng. A* **2019**, *754*, 265–268. [[CrossRef](#)]
37. Wang, Y.; Wu, X.; Cao, L.; Tong, X.; Zou, Y.; Zhu, Q.; Tang, S.; Song, H.; Guo, M. Effect of Ag on aging precipitation behavior and mechanical properties of aluminum alloy 7075. *Mater. Sci. Eng. A* **2021**, *804*, 140515. [[CrossRef](#)]
38. Wang, S.; He, C.; Luo, B.; Bai, Z.; Jiang, G. The role of trace Ag in controlling the precipitation and stress corrosion properties of aluminium alloy 7N01. *Vacuum* **2021**, *184*, 109948. [[CrossRef](#)]
39. Lin, L.; Liu, Z.; Bai, S.; Zhou, Y.; Liu, W.; Lv, Q. Effects of Ge and Ag additions on quench sensitivity and mechanical properties of an Al-Mg-Zn-Cu alloy. *Mater. Sci. Eng. A* **2017**, *682*, 640–647. [[CrossRef](#)]
40. Naeem, H.T.; Mohammed, K.S.; Ahmad, K.R.; Rahmat, A. The Influence of Nickel and Tin Additives on the Microstructural and Mechanical Properties of Al-Zn-Mg-Cu Alloys. *Adv. Mater. Sci. Eng.* **2014**, *2014*, 686474. [[CrossRef](#)]
41. Akopyan, T.K.; Padalko, A.G.; Belov, N.A.; Karpova, Z.A. Effect of Barothermal Treatment on the Structure and the Mechanical Properties of a High-Strength Eutectic Al-Mg-Zn-Cu-Ni Aluminum Alloy. *Russ. Met. (Met.)* **2017**, *2017*, 922–927. [[CrossRef](#)]
42. Liu, F.; Zhu, X.; Ji, S. Effects of Ni on the microstructure, hot tear and mechanical properties of Al-Mg-Zn-Cu alloys under as-cast condition. *J. Alloys Compd.* **2020**, *821*, 153458. [[CrossRef](#)]
43. Zeng, X.C.; Ferguson, C.; Shankar, S. Effect of Titanium levels on the hot tearing sensitivity and abnormal grain growth after T4 treatment of Al-Zn-Mg-Cu alloys. *Int. J. Met.* **2018**, *12*, 457. [[CrossRef](#)]
44. Lee, S.-H.; Jung, J.-G.; Baik, S.-I.; Park, S.H.; Kim, M.-S.; Lee, Y.-K.; Euh, K. Effects of Ti addition on the microstructure and mechanical properties of Al-Mg-Zn-Cu-Zr alloy. *Mater. Sci. Eng. A* **2021**, *801*, 140437. [[CrossRef](#)]
45. Kayani, S.H.; Jung, J.-G.; Kim, M.-S.; Euh, K. Effect of Cooling Rate on Precipitation Behavior of Al-7.65Zn-2.59Mg-1.95Cu Alloy with Minor Elements of Zr and Ti. *Met. Mater. Int.* **2020**, *26*, 1079–1086. [[CrossRef](#)]
46. Lee, S.-H.; Kayani, S.H.; Jung, J.-G.; Baik, S.-I.; Kim, M.-S.; Lee, Y.-K.; Euh, K. Crystallographic characterization of Al₁₈Mg₃Ti₂ intermetallic phase in Al-Mg-Zn-Cu-Zr-Ti alloy. *J. Alloys Compd.* **2020**, *844*, 156173. [[CrossRef](#)]
47. Ying, T.; Gu, L.; Tang, X.; Wang, J.; Zeng, X. Effect of Sc microalloying on microstructure evolution and mechanical properties of extruded Al-Mg-Zn-Cu alloys. *Mater. Sci. Eng. A* **2022**, *831*, 142197. [[CrossRef](#)]
48. Sun, Y.; Pan, Q.; Luo, Y.; Liu, Y.; Sun, Y.; Long, L.; Li, M.; Wang, X.; Liu, S. Study on the primary Al₃Sc phase and the structure heredity of Al-Zn-Mg-Cu-Sc-Zr alloy. *Mater. Charact.* **2020**, *169*, 110601. [[CrossRef](#)]
49. Teng, G.; Liu, C.; Ma, Z.; Zhou, W.; Wei, L.; Chen, Y.; Li, J.; Mo, Y. Effects of minor Sc addition on the microstructure and mechanical properties of 7055 Al alloy during aging. *Mater. Sci. Eng. A* **2018**, *713*, 61–66. [[CrossRef](#)]
50. Mondol, S.; Alam, T.; Banerjee, R.; Kumar, S.; Chattopadhyay, K. Development of a high temperature high strength Al alloy by addition of small amounts of Sc and Mg to 2219 alloy. *Mater. Sci. Eng. A* **2017**, *687*, 221–231. [[CrossRef](#)]
51. Sun, Y.; Luo, Y.; Pan, Q.; Liu, B.; Long, L.; Wang, W.; Ye, J.; Huang, Z.; Xiang, S. Effect of Sc content on microstructure and properties of Al-Zn-Mg-Cu-Zr alloy. *Mater. Today Commun.* **2021**, *26*, 101899. [[CrossRef](#)]
52. Luo, B.; Bai, Z.; Xie, Y. The effects of trace Sc and Zr on microstructure and internal friction of Zn-Al eutectoid alloy. *Mater. Sci. Eng. A* **2004**, *370*, 172–176. [[CrossRef](#)]
53. Jiang, H.; Liu, C.; Ma, Z.; Zhang, X.; Yu, L.; Ma, M.; Liu, R. Fabrication of Al-35Zn alloys with excellent damping capacity and mechanical properties. *J. Alloys Compd.* **2017**, *722*, 138–144. [[CrossRef](#)]
54. Chen, Y.; Liu, C.; Zhang, B.; Ma, Z.; Zhou, W.; Jiang, H.; Huang, H.; Wei, L. Effects of friction stir processing and minor Sc addition on the microstructure, mechanical properties, and damping capacity of 7055 Al alloy. *Mater. Charact.* **2018**, *135*, 25–31. [[CrossRef](#)]

55. Duan, Y.; Xu, G.; Zhou, L.; Xiao, D.; Deng, Y.; Yin, Z.; Peng, B.; Pan, Q.; Wang, Y.; Lu, L. Achieving high superplasticity of a traditional thermal-mechanical processed non-superplastic Al-Zn-Mg alloy sheet by low Sc additions. *J. Alloys Compd.* **2015**, *638*, 364–373. [[CrossRef](#)]
56. Yang, Y.; Tan, P.; Sui, Y.; Jiang, Y.; Zhou, R. Influence of Zr content on microstructure and mechanical properties of As-cast Al-Zn-Mg-Cu alloy. *J. Alloys Compd.* **2021**, *867*, 158920. [[CrossRef](#)]
57. Cassell, A.; Robson, J.; Race, C.; Eggeman, A.; Hashimoto, T.; Besel, M. Dispersoid composition in zirconium containing Al-Zn-Mg-Cu (AA7010) aluminium alloy. *Acta Mater.* **2019**, *169*, 135–146. [[CrossRef](#)]
58. Pan, T.-A.; Tzeng, Y.-C.; Bor, H.-Y.; Liu, K.-H.; Lee, S.-L. Effects of the coherency of Al₃Zr on the microstructures and quench sensitivity of Al-Mg-Zn-Cu alloys. *Mater. Today Commun.* **2021**, *28*, 102611. [[CrossRef](#)]
59. Xiao, Q.-F.; Huang, J.-W.; Jiang, Y.-G.; Jiang, F.-Q.; Wu, Y.-F.; Xu, G.-F. Effects of minor Sc and Zr additions on mechanical properties and microstructure evolution of Al-Zn-Mg-Cu alloys. *Trans. Nonferrous Met. Soc. China* **2020**, *30*, 1429–1438. [[CrossRef](#)]
60. Liu, J.; Yao, P.; Zhao, N.; Shi, C.; Li, H.; Li, X.; Xi, D.; Yang, S. Effect of minor Sc and Zr on recrystallization behavior and mechanical properties of novel Al-Mg-Zn-Cu alloys. *J. Alloys Compd.* **2016**, *657*, 717–725. [[CrossRef](#)]
61. Wang, Y.; Xiong, B.; Li, Z.; Zhang, Y.; Teng, H. Precipitation Behavior of Al₃(Sc,Zr) Particles in High-Alloyed Al-Mg-Zn-Cu-Zr-Sc Alloy During Homogenization. *Arab. J. Sci. Eng.* **2021**, *46*, 6027–6037. [[CrossRef](#)]
62. Jia, M.; Zheng, Z.; Gong, Z. Microstructure evolution of the 1469 Al-Cu-Li-Sc alloy during homogenization. *J. Alloys Compd.* **2014**, *614*, 131–139. [[CrossRef](#)]
63. Liu, C.-Y.; Teng, G.-B.; Ma, Z.-Y.; Wei, L.-L.; Zhang, B.; Chen, Y. Effects of Sc and Zr microalloying on the microstructure and mechanical properties of high Cu content 7xxx Al alloy. *Int. J. Miner. Met. Mater.* **2019**, *26*, 1559–1569. [[CrossRef](#)]
64. Li, Z.; Hu, Z.; Yan, H. Effect of samarium (Sm) addition on microstructure and mechanical properties of Al-5Cu alloys. *J. Wuhan Univ. Technol. Sci. Ed.* **2016**, *31*, 624–629. [[CrossRef](#)]
65. Zhai, F.; Wang, L.; Gao, X.; Feng, Y.; Zhao, S.; Wang, L. Phase evolution of a novel Al-Mg-Zn-Cu-Zr-Sm alloy during homogenization annealing treatment. *Mater. Res. Express* **2020**, *7*, 076518. [[CrossRef](#)]
66. Zhai, F.; Wang, L.; Gao, X.; Zhao, S.; Feng, Y.; Ma, T.; Fan, R. Effect of samarium on the high temperature tensile properties and fracture behaviors of Al-Mg-Zn-Cu-Zr alloy. *Mater. Res. Express* **2021**, *8*, 016521. [[CrossRef](#)]
67. Zhai, F.; Fan, R.; Feng, Y.; Wang, L. Effect of samarium modification on the microstructures evolution and mechanical properties of high strength aluminum alloy. *Mater. Character.* **2022**, *194*, 112349. [[CrossRef](#)]
68. Fang, H.; Chao, H.; Chen, K. Effect of Zr, Er and Cr additions on microstructures and properties of Al-Mg-Zn-Cu alloys. *Mater. Sci. Eng. A* **2014**, *610*, 10–16. [[CrossRef](#)]
69. Zhong, H.; Li, S.; Zhang, Z.; Li, D.; Deng, H.; Chen, J.; Qi, L.; Ojo, O.A. Precipitation behavior, mechanical properties, and corrosion resistance of rare earth-modified Al-Zn-Mg-Cu alloys. *Mater. Today Commun.* **2022**, *31*, 103732. [[CrossRef](#)]
70. Krishnan, A.; Raja, V.; Mukhopadhyay, A. Influence of Retrogression and Re-aging on the Exfoliation Corrosion Behavior of AA 7085 Sheets. *Corros. Sci. Technol.* **2016**, *15*, 159–165. [[CrossRef](#)]
71. Wang, Y.; Wu, X.; Cao, L.; Tong, X.; Couper, M.J.; Liu, Q. Effect of trace Er on the microstructure and properties of Al-Mg-Zn-Cu-Zr alloys during heat treatments. *Mater. Sci. Eng. A* **2020**, *792*, 139807. [[CrossRef](#)]
72. Chen, Z.-Q.; Hu, W.-X.; Shi, L.; Wang, W. Effect of rare earth on morphology and dispersion of TiB₂ phase in Al-Ti-B alloy refiner. *China Foundry* **2023**, *20*, 115–124. [[CrossRef](#)]
73. Yin, D.S.; Zhang, N.; Chen, K.J.; Zhang, Y.L. Effect of Gd on microstructure and refinement performance of Al-5Ti-B alloy. *China Foundry* **2021**, *18*, 223. [[CrossRef](#)]
74. Wang, Z.; Xiao, H.; Ma, L.; Fan, T.; Tang, P. Effects of rare-earth elements on twinning deformation of Al alloys from first-principles calculations. *Solid State Commun.* **2022**, *356*, 114946. [[CrossRef](#)]
75. Zhai, F.; Wang, L.; Gao, X.; Feng, Y.; Zhao, S.; Wang, L. Study on Phases Formation and Modification Ability of Rare Earth Elements La, Ce, Sm and Er in Al-Mg-Zn-Cu-Zr Alloy. *Trans. Indian Inst. Met.* **2021**, *74*, 2639–2649. [[CrossRef](#)]
76. Yu, X.-X.; Sun, J.; Li, Z.-T.; Dai, H.; Fang, H.-J.; Zhao, J.-F.; Yin, D.-F. Solidification behavior and elimination of undissolved Al₂CuMg phase during homogenization in Ce-modified Al-Mg-Zn-Cu alloy. *Rare Met.* **2020**, *39*, 1279–1287. [[CrossRef](#)]
77. Michalik, R.; Woźnica, H. The Effect of Ti and REE Addition on the Corrosion Resistance of the AlZn₁₂Mg_{3.5}Cu_{2.5} Alloy in “Acid Rain” Environment. *Solid State Phenom.* **2015**, *227*, 111–114. [[CrossRef](#)]
78. Hu, G.; Zhu, C.; Xu, D.; Dong, P.; Chen, K. Effect of cerium on microstructure, mechanical properties and corrosion properties of Al-Zn-Mg alloy. *J. Rare Earths* **2021**, *39*, 208–216. [[CrossRef](#)]
79. Wang, M.; Knezevic, M.; Chen, M.; Li, J.; Liu, T.; Wang, G.; Zhao, Y.; Wang, M.; Liu, Q.; Huang, Z.; et al. Microstructure design to achieve optimal strength, thermal stability, and electrical conductivity of Al-7.5wt.%Y alloy. *Mater. Sci. Eng. A* **2022**, *852*, 143700. [[CrossRef](#)]
80. Ding, W.; Zhao, X.; Chen, T.; Zhang, H.; Liu, X.; Cheng, Y.; Lei, D. Effect of rare earth Y and Al-Ti-B master alloy on the microstructure and mechanical properties of 6063 aluminum alloy. *J. Alloys Compd.* **2020**, *830*, 154685. [[CrossRef](#)]
81. Li, J.; Zhang, Y.; Li, M.; Hu, Y.; Zeng, Q.; Zhang, P. Effect of combined addition of Zr, Ti and Y on microstructure and tensile properties of an Al-Zn-Mg-Cu alloy. *Mater. Des.* **2022**, *223*, 111129. [[CrossRef](#)]
82. Yang, W.; Pang, M.; Tan, Y.; Zhan, Y. A comparative first-principles study on electronic structures and mechanical properties of ternary intermetallic compounds Al₈Cr₄Y and Al₈Cu₄Y: Pressure and tension effects. *J. Phys. Chem. Solids* **2016**, *98*, 298–308. [[CrossRef](#)]

83. Zhang, D.; Qiu, D.; Gibson, M.A.; Zheng, Y.; Fraser, H.L.; StJohn, D.H.; Easton, M.A. Additive manufacturing of ultrafine-grained high-strength titanium alloys. *Nature* **2019**, *576*, 91–95. [[CrossRef](#)] [[PubMed](#)]
84. Martin, J.H.; Yahata, B.; Mayer, J.; Mone, R.; Stonkevitch, E.; Miller, J.; O'Masta, M.R.; Schaedler, T.; Hundley, J.; Callahan, P.; et al. Grain refinement mechanisms in additively manufactured nano-functionalized aluminum. *Acta Mater.* **2020**, *200*, 1022–1037. [[CrossRef](#)]
85. Straumal, B.; Baretzky, B.; Mazilkin, A.; Phillipp, F.; Kogtenkova, O.; Volkov, M.; Valiev, R. Formation of nanograined structure and decomposition of supersaturated solid solution during high pressure torsion of Al-Zn and Al-Mg alloys. *Acta Mater.* **2004**, *52*, 4469–4478. [[CrossRef](#)]
86. Li, X.; Li, D.; Li, G.; Cai, Q. Microstructure, mechanical properties, aging behavior, and corrosion resistance of a laser powder bed fusion fabricated Al-Mg-Zn-Cu-Ta alloy. *Mater. Sci. Eng. A* **2022**, *832*, 142364. [[CrossRef](#)]
87. Won, S.-J.; So, H.; Han, J.-W.; Oh, S.J.; Kang, L.; Kim, K.-H. Effects of Sc and Be Microalloying Elements on Mechanical Properties of Al-Zn-Mg-Cu (Al7xxx) Alloy. *Metals* **2023**, *13*, 340. [[CrossRef](#)]
88. Won, S.-J.; So, H.; Han, J.-W.; Oh, S.J.; Kim, K.-H. Roles of Sc and Ag Microalloying Elements in the Mechanical Properties of Al-Zn-Mg-Cu (Al7xxx) Alloy. *Metals* **2023**, *13*, 244. [[CrossRef](#)]

Disclaimer/Publisher's Note: The statements, opinions and data contained in all publications are solely those of the individual author(s) and contributor(s) and not of MDPI and/or the editor(s). MDPI and/or the editor(s) disclaim responsibility for any injury to people or property resulting from any ideas, methods, instructions or products referred to in the content.